Deep-Sea Research I 58 (2011) 111–127

Contents lists available at ScienceDirect

Deep-Sea Research I

journal homepage: www.elsevier.com/locate/dsri

# Biogeochemistry and carbon mass balance of a coccolithophore bloom in the northern Bay of Biscay (June 2006)

J. Harlay [a,b,*], L. Chou [a], C. De Bodt [a], N. Van Oostende [c], J. Piontek [d], K. Suykens [b], A. Engel [d], K. Sabbe [c], S. Groom [e], B. Delille [b], A.V. Borges [b]

[a] Laboratoire d'Océanographie Chimique et Géochimie des Eaux, Université Libre de Bruxelles, Campus de la Plaine, CP208, boulevard du Triomphe, B-1050 Brussels, Belgium
[b] Chemical Oceanography Unit, Université de Liège, Institut de Physique (B5), B-4000 Sart Tilman, Belgium
[c] Protistology and Aquatic Ecology, Gent University, Krijgslaan 281-S8, B-9000 Gent, Belgium
[d] HGF Young Investigators Group, Global change and the future marine carbon cycle, Alfred Wegener Institute, Am Handelshafen 12, D-27570 Bremerhaven, Germany
[e] Remote Sensing Group, Plymouth Marine Laboratory, Prospect Place, West Hoe, Plymouth PL1 3DH, United Kingdom

ARTICLE INFO

*Article history:*
Received 20 August 2010
Received in revised form
12 November 2010
Accepted 18 November 2010
Available online 24 November 2010

*Keywords:*
Bay of Biscay
Coccolithophores
*Emiliania huxleyi*
Primary production
Calcification
Dark community respiration
$CO_2$ fluxes

ABSTRACT

Primary production (PP), calcification (CAL), bacterial production (BP) and dark community respiration (DCR) were measured along with a set of various biogeochemical variables, in early June 2006, at several stations at the shelf break of the northern Bay of Biscay. The cruise was carried out after the main spring diatom bloom that, based on the analysis of a time-series of remotely sensed chlorophyll-a (Chl-a), peaked in mid-April. Remotely sensed sea surface temperature (SST) indicated the occurrence of enhanced vertical mixing (due to internal tides) at the continental slope, while adjacent waters on the continental shelf were stratified, as confirmed by vertical profiles of temperature acquired during the cruise. The surface layer of the stratified water masses (on the continental shelf) was depleted of inorganic nutrients. Dissolved silicate (DSi) levels probably did not allow significant diatom development. We hypothesize that mixing at the continental slope allowed the injection of inorganic nutrients that triggered the blooming of mixed phytoplanktonic communities dominated by coccolithophores (*Emiliania huxleyi*) that were favoured with regards to diatoms due to the low DSi levels. Based on this conceptual frame, we used an indicator of vertical stratification to classify the different sampled stations, and to reconstruct the possible evolution of the bloom from the onset at the continental slope (triggered by vertical mixing) through its development as the water mass was advected on-shelf and stratified. We also established a carbon mass balance at each station by integrating in the photic layer PP, CAL and DCR. This allowed computation at each station of the contribution of PP, CAL and DCR to $CO_2$ fluxes in the photic layer, and how they changed from one station to another along the sequence of bloom development (as traced by the stratification indicator). This also showed a shift from net autotrophy to net heterotrophy as the water mass aged (stratified), and suggested the importance of extracellular production of carbon to sustain the bacterial demand in the photic and aphotic layers.



## 1. Introduction

During coccolithophore blooms, carbon (C, all abbreviations are defined in Table 1) cycling in the photic zone is driven by the production and degradation of organic matter (primary production (PP) and community respiration), and the production and dissolution of biogenic calcite ($CaCO_3$). Both processes transfer C to depth and impact on the speciation of dissolved inorganic C (DIC) and $CO_2$ flux across the air–sea interface (Purdie and Finch, 1994; Buitenhuis et al., 1996, 2001; Crawford and Purdie, 1997; Frankignoulle and Borges, 2001; Suykens et al., 2010a). Changes of C fluxes of pelagic calcifiers under ocean acidification (e.g., Orr et al., 2005), namely a decrease in calcification rates, could provide a negative feedback in response to increasing atmospheric $CO_2$ as suggested by controlled experiments either in cultures (e.g., Riebesell et al., 2000; Sciandra et al., 2003; De Bodt et al., 2008, 2010) or mesocosms (e.g., Delille et al., 2005; Riebesell et al., 2007). Further, due to their relatively large contribution to the phytoplanktonic community, and their complex life cycle which alternates between naked and calcified forms, the effect of coccolithophores on $CO_2$ fluxes is variable during bloom development, altering the ratio of calcification (CAL) to PP (Billard and Inouye, 2004). Understanding and quantifying the C cycling associated with coccolithophore blooms under natural conditions is needed to correctly parameterize and validate biogeochemical

* Corresponding author at: Chemical Oceanography Unit, Université de Liège, Institut de Physique (B5), B-4000 Sart Tilman, Belgium.
*E-mail address:* jerome.harlay@ulg.ac.be (J. Harlay).

0967-0637/$ - see front matter © 2010 Elsevier Ltd. All rights reserved.
doi:10.1016/j.dsr.2010.11.005

**Table 1**
List and definition of abbreviations used in text.

| Abbreviation | Definition |
|---|---|
| $\%O_2$ | Oxygen saturation |
| AVHRR | Advanced very high resolution radiometer |
| BOD | Biological oxygen demand |
| BP | Bacterial production |
| C | Carbon |
| $CaCO_3$ | Calcium carbonate |
| CAL | Calcification |
| Chl-a | Chlorophyll-a |
| $CO_2$ | Carbon dioxide |
| CTD | Conductivity-temperature-depth |
| DCR | Dark community respiration |
| DIC | Dissolved inorganic carbon |
| DSi | Dissolved silicate concentration |
| GPP | Gross primary production |
| HPLC | High performance liquid chromatography |
| HR | High reflectance |
| $K_d$ | Diffuse attenuation coefficient |
| $L_{wn}(555)$ | Normalized water-leaving radiance at 555 nm |
| MLD | Mixed layer depth |
| MODIS | Moderate-resolution imaging spectrometer |
| NMCF | Net metabolic carbon flux |
| NCP | Net community production |
| $O_2$ | Oxygen |
| PAR | Photoysynthetically active radiation |
| $pCO_2$ | Partial pressure of carbon dioxide |
| PIC | Particulate inorganic carbon |
| $PO_4$ | Phosphate concentration |
| POC | Particulate organic carbon |
| PP | Primary production |
| $PP_d$ | Dissolved primary production |
| $PP_{tot}$ | Total primary production |
| SeaWIFs | Sea-viewing Wide Field-of-view Sensor |
| SST | Sea surface temperature |
| TCA | Trichloroacetic acid |
| TEP | Transparent exopolymer particles |
| TEP-C | Transparent exopolymer particles carbon concentration |
| TPC | Total particulate carbon |
| UML | Upper mixed layer |

models that aim at predicting feedbacks related to ocean acidification and incorporate knowledge obtained from perturbation laboratory experiments.

Coccolithophore blooms have an identifiable spectral signature (reflectance) on the 555 nm band from remote sensing (Balch et al., 2005, 2007; Balch and Utgoff, 2009) and have frequently been observed in the English Channel (GREPMA, 1988; Garcia-Soto et al., 1995), the Celtic Sea and the Bay of Biscay (Holligan et al., 1983; Garcia-Soto and Pingree, 2009; Harlay et al., 2010; Suykens et al., 2010a) from high reflectance (HR) patches on satellite images. These HR patches have been attributed to blooms of the coccolithophore *Emiliania huxleyi*, which can reach concentrations above $10^8$ liths $L^{-1}$ (Holligan et al., 1993).

We carried out a survey at the continental margin of the northern Bay of Biscay in early June 2006 when a HR patch associated with a coccolithophore bloom was observed. We report physico-chemical and biogeochemical parameters (temperature, nutrients, chlorophyll-a (Chl-a), and oxygen saturation ($\%O_2$)), elemental composition of suspended particulate matter as well as community metabolic rates like the daily rates of CAL, PP, bacterial production (BP), and dark community respiration (DCR). Remotely sensed images and the output of a physical model were used to analyse the seasonal phytoplankton dynamics. Finally, based on community metabolic rate measurements, we compute and discuss a C mass balance for the photic zone.

## 2. Materials and methods

### 2.1. Study site

The study area is at the shelf break of the Celtic Sea in the northern Bay of Biscay, located in the eastern North Atlantic Ocean (Fig. 1). The topography of the shelf-edge of the northern Bay of Biscay defines the particular physical conditions at the La Chapelle Bank and the Meriadzek Terrace: combined to strong tidal currents,

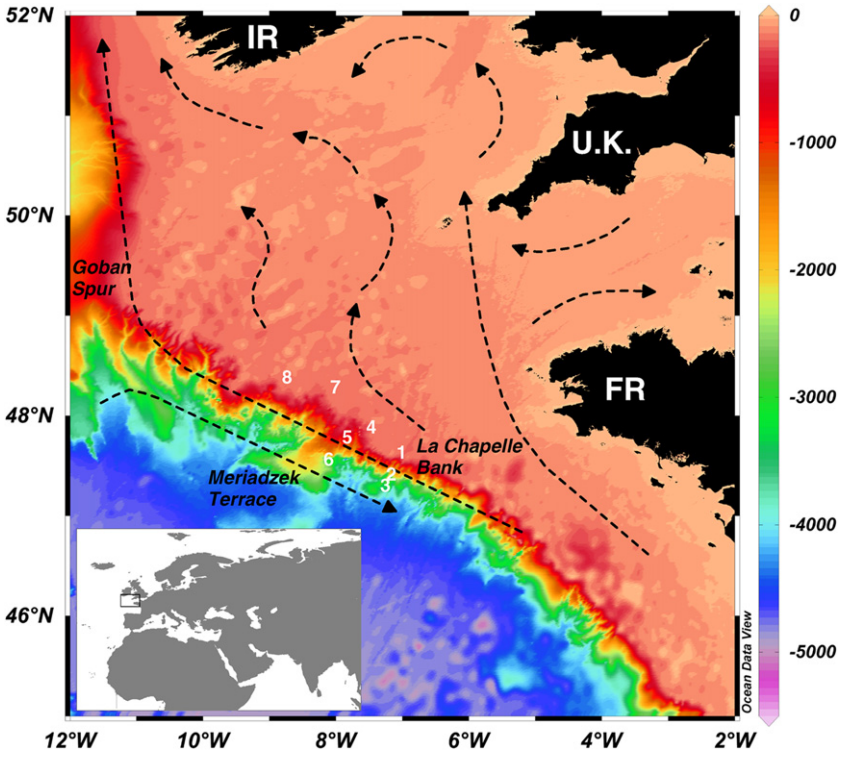


**Fig. 1.** Map of the northern Bay of Biscay showing bathymetry (Smith and Sandwell, 1997), the location of the stations and surface currents (Pingree and Le Cann, 1989; Pingree, 1993; Pingree et al., 1999 and Huthnance et al., 2001). The stations 1 and 4 were revisited after 9 and 6 days, respectively, and referred to as 1bis and 4bis in the text.

the steep slope enhances shear stress and generates internal tides and turbulence which favours vertical mixing (Pingree and New, 1995). These hydrographic properties are evidenced by the distribution of sea surface temperature (SST) on satellite images, where a cold patch of water streches during spring and summer, when sufficient stratification has developed, between the 200 m and the 2000 m isobaths (Wollast and Chou, 2001). The vertical mixing occurs by pulses at the shelf break and erodes the seasonal thermocline leading to the upward transport of deeper water, sustaining biological activity during spring and summer by supplying nutrients to the photic zone (Pingree et al., 1986; Joint et al., 2001; Wollast and Chou, 2001; Sharples et al., 2007, 2009). Sharples et al. (2007) showed that during spring tides, enough nitrate pulses are released to the photic zone to sustain new production of phytoplankton and to induce shifts in the plankton community on a fortnighly basis (spring and neap tide oscillations). The use of phytoplankton pigments used as biomarkers indicates that the most abundant taxa are prymnesiophytes, among which the coccolithophore *E. huxleyi*, with two short blooms of diatoms in spring and fall (Joint et al., 2001). Along-slope currents northwestern winds contribute to the advection of surface waters and general cross-slope water motion (Huthnance et al., 2001; Sharples et al., 2007).

### 2.2. Sampling strategy

Samples were collected at the continental margin between 31 May and 9 June 2006 (Fig. 1; Table 2). The cruise was split into two legs (first leg: 31st May to 3rd June; second leg: 5th June to 9th June), during which two stations (1 and 4) were revisited after 9 and 6 days, respectively, and named 1bis and 4bis. The stations were located over the continental shelf at depths $<180$ m (stations 1, 4, 7 and 8) and along the shelf break and slope at depths of $\sim$600 m (stations 2 and 5) and $\sim$1600 m (stations 3 and 6).

### 2.3. Vertical hydrography and light attenuation

A Seabird CTD (SBE21), with a rosette sampler of 12 Niskin bottles (10 L), was used to determine vertical profiles of temperature and salinity, and to collect seawater for chemical and biological analyses. At each station, water was collected at dawn at 3, 20, 40, 60, 80, 100 and 150 m depth. Vertical profiles of *in situ* photosynthetic active radiation (PAR) were acquired in the water column with a Seabird SBE19 equipped with a LiCor Li-192-SA PAR sensor, around noon for each station. From the PAR profile, the downwelling diffuse attenuation coefficient $K_d$ ($m^{-1}$) and the photic depth (corresponding to 1% of the incoming PAR) were determined.

### 2.4. Inorganic nutrients

Samples were filtered through 0.4 μm Nuclepore filters and preserved at $-20$ °C for total phosphate ($PO_4$) and 4 °C for dissolved silicate (DSi) until analysis. Seawater $PO_4$ and DSi concentrations were measured colorimetrically with the molybdate/ascorbic acid method (Grasshoff et al., 1983).

### 2.5. Photosynthetic pigments concentration

#### 2.5.1. Fluorometric determination of Chl-a

Chl-a concentration was determined fluorometrically according to Yentsch and Menzel (1963): 250 ml of seawater was filtered through a glass fibre filter (47 mm Whatman GF/F) which was then wrapped in aluminium foil and stored on board at $-20$ °C before analysis. Extraction of pigments was carried out overnight at $-20$ °C in the dark, in 10 ml 90% acetone and centrifuged for 10 min at 5000 rpm before the fluorescence measurement with a Shimatzu RF-1501 spectrofluorophotometer.

#### 2.5.2. High performance liquid chromatographic (HPLC) determination of pigments

About 500–3500 ml of seawater was filtered through glass fibre filters (47 mm Whatman GF/F) that were subsequently stored in liquid nitrogen onboard the ship and during transport. Extraction of the pigments was performed in 90% acetone. The frozen filters were cut into small pieces (several mm $\times$ 1 cm) and sonicated (pulses) for 30 s (50 W) in a centrifuge tube with 3.5 ml 90% acetone. The extracts were cleared from debris by filtering through a 0.2 μm Teflon syringe filter after centrifuging at $-5$ °C for 4 min at 700*g*. The HPLC method, based on Wright and Jeffrey (1997), allowed separation of the different pigments that were used to estimate the

**Table 2**
Stations, sampling date, location, depth, MLD (in m), photic depth, SST (°C), $pCO_2$ (μatm, from Suykens et al., 2010a) and $\%O_2$ (%), $PO_4$ and DSi concentrations (μmol $L^{-1}$) in surface waters, integrated concentration of Chl-a (mg $m^{-2}$), POC and PIC (in g C $m^{-2}$), PIC:POC ratio, integrated rates in the photic zone of PP, CAL, BP (mg C $m^{-2}$ $d^{-1}$), DCR (mmol $O_2$ $m^{-2}$ $d^{-1}$), and CAL:PP ratio in the northern Bay of Biscay in June 2006 (the cruise was split into two legs: first leg from 31st May to 3rd June; second leg from 5th June to 9th June). Some of the variables were not determined at some stations ("nd").

| Station | | 1 | 1bis | 2 | 3 | 4 | 4bis | 5 | 6 | 7 | 8 |
|---|---|---|---|---|---|---|---|---|---|---|---|
| Date | | 31/05/2006 | 09/06/2006 | 01/06/2006 | 01/06/2006 | 02/06/2006 | 08/06/2006 | 02/06/2006 | 07/06/2006 | 07/06/2006 | 06/06/2006 |
| Latitute | (°N) | 47.7488 | 47.7499 | 47.5330 | 47.4168 | 48.0999 | 48.0997 | 47.9011 | 47.6786 | 48.3997 | 48.5003 |
| Longitude | (°W) | 7.0000 | 7.0010 | 7.1661 | 7.2651 | 7.5016 | 7.4999 | 7.9015 | 8.2093 | 8.0993 | 8.9011 |
| Depth | (m) | 157 | 158 | 680 | 1826 | 162 | 167 | 527 | 1248 | 164 | 180 |
| MLD | (m) | 32 | 22 | 40 | 21 | 34 | 23 | 53 | 16 | 20 | 19 |
| photic depth | (m) | 30 | 37 | 31 | nd | 26 | 27 | nd | nd | 27 | 34 |
| SST | (°C) | 13.03 | 14.34 | 12.99 | 13.98 | 13.29 | 14.20 | 13.25 | 14.86 | 14.51 | 14.48 |
| $pCO_2$ | (μatm) | 265 | 273 | 306 | 323 | 293 | 307 | 353 | 324 | 309 | 325 |
| $\%O_2$ | (%) | 111 | 111 | 110 | 110 | 108 | 109 | 106 | 116 | 110 | 110 |
| $PO_4$ | (μmol $L^{-1}$) | 0.00 | 0.03 | 0.08 | 0.46 | 0.04 | 0.04 | 0.12 | 0.04 | 0.01 | 0.04 |
| DSi | (μmol $L^{-1}$) | 0.59 | 0.25 | 1.40 | 0.00 | 0.33 | 0.45 | 0.62 | 0.48 | 0.45 | 1.65 |
| Integrated Chl-a | (mg Chl-a $m^{-2}$) | 90.2 | 36.6 | 130.3 | nd | 50.5 | 57.1 | 74.8 | nd | 48.3 | 34.9 |
| Integrated POC | (g C $m^{-2}$) | 9.24 | 8.95 | 10.29 | nd | 6.93 | 4.40 | nd | nd | 10.46 | 8.56 |
| Integrated PIC | (g C $m^{-2}$) | 6.64 | 2.48 | 8.04 | nd | 2.39 | 2.65 | nd | nd | 2.40 | 4.34 |
| PIC:POC | | 0.72 | 0.28 | 0.78 | nd | 0.34 | 0.60 | nd | nd | 0.23 | 0.51 |
| Integrated PP | (mg C $m^{-2}$ $d^{-1}$) | 950 | 710 | 2160 | nd | 650 | 660 | 1170 | nd | 900 | 430 |
| Integrated CAL | (mg C $m^{-2}$ $d^{-1}$) | 90 | 190 | 620 | nd | 160 | 150 | 290 | nd | 430 | 160 |
| CAL:PP | | 0.09 | 0.27 | 0.29 | nd | 0.24 | 0.23 | 0.25 | nd | 0.48 | 0.38 |
| Integrated BP | (mg C $m^{-2}$ $d^{-1}$) | 116 | nd | 48 | nd | 51 | nd | nd | nd | 53 | 47 |
| Integrated DCR | (mmol $O_2$ $m^{-2}$ $d^{-1}$) | 73.7 | 103.5 | 81.3 | nd | 78.9 | 101.2 | nd | nd | 81.4 | 104.3 |

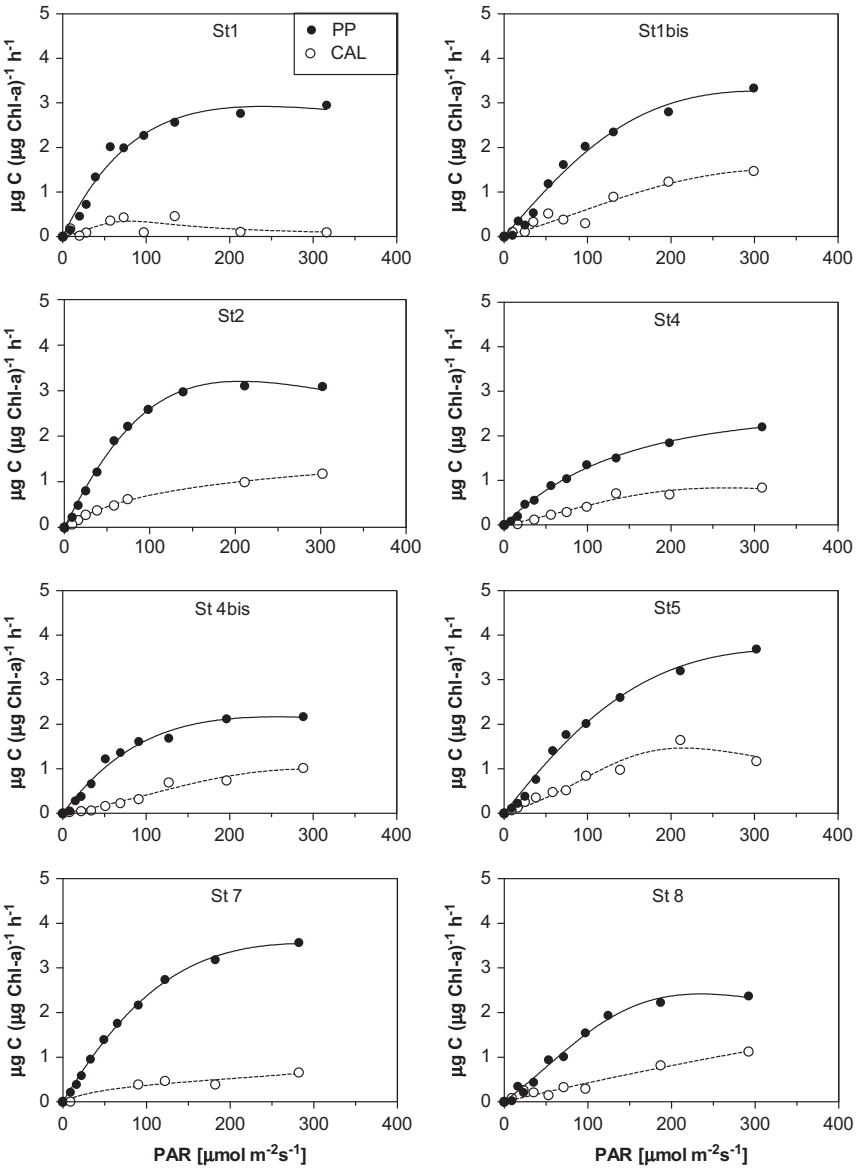


**Fig. 2.** Chl-a normalized $^{14}C$ primary production (PP, µg C (µg Chl-a)$^{-1}$ h$^{-1}$) and calcification (CAL, µg C (µg Chl-a)$^{-1}$ h$^{-1}$) versus irradiance (PAR, µmol m$^{-2}$ s$^{-1}$) in surface waters in northern Bay of Biscay in June 2006.

taxonomic composition of the phytoplankton community, expressed in % of total Chl-a for each phytoplankton group, according to the Bayesian Compositional Estimator (Van den Meersche et al., 2008). Standard pigment mixtures were used to allow identification and quantification of the detected pigment peaks in the chromatogram.

Fluorometric Chl-a was sampled with a higher vertical resolution than HPLC Chl-a; hence, hereafter, only the fluorometric Chl-a are shown and discussed, while the HPLC pigment data are used to discuss the taxonomic composition of phytoplankton.

### 2.6. Particulate organic (POC) and inorganic (PIC) carbon

Seawater (200–2000 ml) was filtered onto duplicate precombusted (4 h, 500 °C) 25 mm Whatman GF/F filters. The samples were stored at −20 °C until analysis. Within three months after the cruise, the filters were dried overnight at 50 °C. One set of the duplicate filters was acidified overnight under HCl fumes at room temperature in order to remove inorganic carbon. The filtered area was stamped out with a calibrated punch in order to remove the external ring of the filter. Filters were packed in solvent-rinsed tin sample boats for analysis. The POC and the total particulate carbon (TPC) concentrations in the suspended matter were determined sequentially with a Fisons NA-1500 CHN microanalyzer. The PIC concentration was calculated by difference between TPC and POC. Five standards (STSD2, certified reference stream sediment from the Geological survey of Canada) and four blanks were used to derive the calibration with least-squares regression.

### 2.7. Processes measurements

#### 2.7.1. $^{14}C$ primary production and calcification

PP and CAL were determined following the protocol given by Harlay et al. (2010) using an incubation period of 4 h. At each station, the response of PP and CAL to irradiance (PAR) (PP versus PAR and CAL versus PAR curves) were determined at the surface (3 m depth; Fig. 2) and integrated versus depth and time to determine daily rates of PP and CAL (Table 2).

*2.7.2. Bacterial production*

Bacterial production was determined by the incorporation of $^{3}$[H]-thymidine. Samples (10–20 ml) were incubated in duplicate with 10 nM of $^{3}$[H]-thymidine for 90 min in the dark close to *in situ* temperature. After incubation, samples were poisoned with 2% formalin and filtered on 0.2 μm polycarbonate filters. According to Fuhrman and Azam (1982), samples were rinsed with ice-cold 5% TCA and radio-assayed by liquid scintillation counting with Ultima Gold AB as scintillation cocktail. To calculate bacterial biomass production from thymidine incorporation, a conversion factor of $1.74 \times 10^{18}$ cells mol$^{-1}$ incorporated thymidine with an average cell volume of 0.03 μm$^3$ was assumed (Kirchman, 1992). Furthermore, a carbon conversion factor of $0.3 \times 10^{-6}$ μg C μm$^{-3}$ cell$^{-1}$ was used (Fuhrman and Azam, 1982).

*2.8. Pelagic dark community respiration (DCR) and dissolved oxygen saturation (%$O_2$)*

Water samples were collected from Niskin bottles in biological oxygen demand (BOD) bottles. Concentration of dissolved $O_2$ was measured by automated Winkler titration with potentiometric end-point detection using a Metrohm redox electrode (6.0451.100) and Metrohm titrator (Dosimat 625). Reagents and standardizations were similar to those described by Knap et al. (1996). The saturation concentration of seawater with respect to oxygen was computed with the algorithm given by Benson and Krause (1984).

DCR measurement was determined on 3 replicates (60 ml BOD bottles) fixed immediately after collection with the Winkler reagents while 3 other replicates were incubated for 24 h in the dark, cooled with running seawater pumped from 2.5 m depth. Dissolved $O_2$ in the water column was determined on 50 ml subsamples from a 300 ml BOD bottle.

*2.9. Integration of the data*

As a way of reconstructing the bloom sequence and succession of the mixed phytoplankton community, and showing how this creates an ecological niche favourable for coccolithophores, available biogeochemical parameters and processes were plotted against the difference of seawater density between 100 and 3 m ($\Delta\rho_{100\ m-3\ m}$). The $\Delta\rho_{100\ m-3\ m}$ values are used as indicators of the degree of stratification of the water column, and this approach was preferred because it is easily computed and is sufficient for the purpose of the analysis. The use of mixed layer depth (MLD) as a descriptor for stratification gave similar patterns as $\Delta\rho_{100\ m-3\ m}$ (not shown).

## 3. Results

*3.1. Seasonal evolution of key remotely sensed biological and modelled physical variables*

Time-series from late winter to late summer 2006 of remotely sensed Chl-a, and normalized water-leaving radiance at 555 nm ($L_{wn}$(555)), and modelled key physical variables (upper mixed layer (UML) and SST) were used to set our cruise in the frame of the overall seasonal cycle of phytoplankton biomass, and the physical conditions prevailing in the area before and after the cruise. Chl-a increased rapidly in early April 2006 with the onset of the spring bloom and peaked in mid-April (Fig. 3), in agreement with previous observations in the area (Wollast and Chou, 2001; Hydes et al., 2001; Joint et al., 2001). A second peak of Chl-a was observed three weeks later, after which Chl-a concentration decreased, and remained low from early July onwards. After the second peak of Chl-a, $L_{wn}$(555) representing the backscatter of suspended calcite, hence of the coccolithophore cells and liths, increased by 3-fold from winter values (0.3–0.5 mW cm$^{-2}$ μm$^{-1}$ sr$^{-1}$) to peak in mid-May (~1.1 mW cm$^{-2}$ μm$^{-1}$ sr$^{-1}$) one week before our cruise, and decreased to background level in late June. In mid-April, SST started to increase from the winter value (~11 °C), coinciding with the first peak of Chl-a. The UML depth started shoaling in mid-April to attain, in mid-May, a value of ~35 m, corresponding to the depth of the photic layer. $L_{wn}$(555) started to increase when the mixed layer depth attained a value of ~35 m, to peak about three weeks later, in mid-May, concomitantly to an increase of SST. A deepening of the UML and a decrease of SST occurred just before the start of the cruise, due to stormy weather, and coincided with a decrease of $L_{wn}$(555). The possible scenario underlying this decrease of $L_{wn}$(555) is a mixing of surface water and a redistribution of the

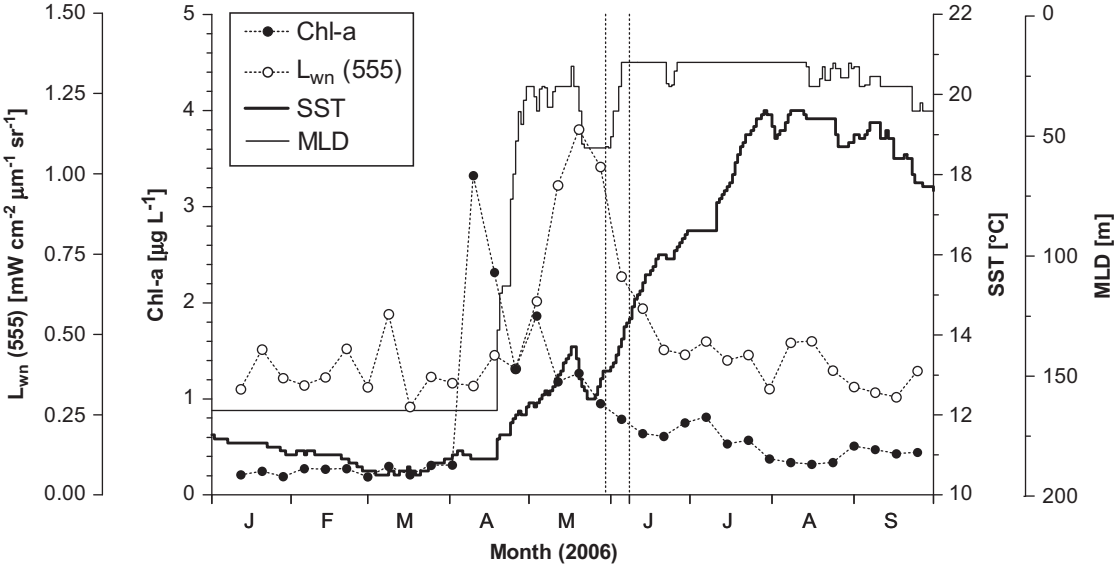


**Fig. 3.** Time series from January to September 2006 of remotely sensed weekly Chl-a concentrations (μg L$^{-1}$) (left axis) and $L_{wn}$ (555) (mW cm$^{-2}$ μm$^{-1}$ sr$^{-1}$; left axis), modelled MLD (m; right axis) and SST (°C; right axis) for a box in in the northern Bay of Biscay [48.5°–48.0°N; 8.0°–7.5°W]. The vertical dotted lines correspond to the period of the cruise (31 May to 9 June 2006). Chl-an and $L_{wn}$ (555) are Level-3 Sea-viewing Wide Field-of-view Sensor data (http://reason.gsfc.nasa.gov/Giovanni/), and MLD and SST were simulated by Met Office National Centre for Ocean Forecasting for the North-East Atlantic 1/8° model.

suspended matter through the water column. The period of the cruise coincided with a period of thermal re-stratification with an increase of SST and a shoaling of the UML depth that remained close to 25 m until September as SST increased up to 19 °C.

### 3.2. Biogeochemical settings in June 2006

The cruise was carried out with the support of near-real time remotely sensed images of SST, Chl-a and reflectance (Fig. 4). Along the shelf break, several patches of cold water (SST < 14 °C) were observed in the studied area (Fig. 4a), corresponding to the signature of enhanced vertical mixing due to internal tides (Pingree et al., 1999; Wollast and Chou 2001). These patches of cold waters were characterized by lower Chl-a levels (~0.4 μg $L^{-1}$) and were surrounded by waters exhibiting higher Chl-a values (> 0.8 μg $L^{-1}$) on-shelf and off-shore (Fig. 4b). This was related to the propagation of these nutrient rich colder waters from the shelf-break off- and on-shore due to baroclinic eddy activity along the edges of the cold water patch (Sharples et al., 2007, 2009; Jonathan Sharples, pers. comm., 2010), leading to enhanced biological activity as they warm and stratify. As these water-masses propagated further on the shelf, phytoplankton activity caused nutrient exhaustion and solar irradiance induced a warming leading to stratification. Hence, the high Chl-a waters were confined close to the shelf-break (Fig. 4b). The sampled stations were located in relatively warm areas (SST > 13 °C) characterized by moderate (0.80 μg $L^{-1}$; station 8) to higher (1.62 μg $L^{-1}$; station 6) Chl-a values. Several HR patches associated with moderate Chl-a concentrations were located on-shelf bordering the shelf-break, clustered mainly around 50°N and 48°N (Fig. 4c). Our sampling stations were distributed within and around a HR patch that was centred at the location of station 4.

The vertical profiles of temperature in Fig. 5 agree with remotely sensed SST (Fig. 4a), with temperatures in surface waters ranging from 13.0 to 14.0 °C (Table 2) during the first leg (stations 1–5). An increase of ~1 °C was observed during the second leg, with SST values ranging from 14.2 to 14.9 °C (stations 6, 7, 8, 4bis and 1bis). The upper part of the water column was stratified with MLD ranging between 20 and 80 m (Fig. 5; Table 2). Stations located on the continental slope (2 and 5) showed less stratification due to enhanced vertical mixing related to internal tides (Pingree et al., 1999; Wollast and Chou 2001). Stratification increased from the first to the second leg. The photic depth ranged between 26 and 37 m (stations 7 and 1bis, respectively; Table 2).

Surface waters were depleted in $PO_4$ with concentrations below or close to 0.1 μmol $L^{-1}$ at all stations except station 3 (Fig. 6). The $PO_4$ concentration increased with depth to 0.5 μmol $L^{-1}$ below the photic zone. DSi exhibited a lesser depletion than $PO_4$ but concentrations remained below 2.0 μmol $L^{-1}$ in the UML. DSi concentrations in surface waters were close to 0.6 μmol $L^{-1}$, except at stations 2 and 8, where values ~1.5 μmol $L^{-1}$ were measured (Fig. 6).

Chl-a concentration profiles exhibited higher values in the photic zone, ranging between 0.2 μg $L^{-1}$ (station 1bis) and 2.0 μg $L^{-1}$ (station 2; Fig. 7). Station 2 showed the highest Chl-a concentration with values > 1.0 μg $L^{-1}$ down to 60 m depth. At station 8, Chl-a concentration was lower than 1.0 μg $L^{-1}$ over the entire water column. The vertical distribution of Chl-a at the revisited stations showed a decrease of 40–50% in surface waters and a deepening of the sub-surface maximum to the bottom of the UML (stations 1bis

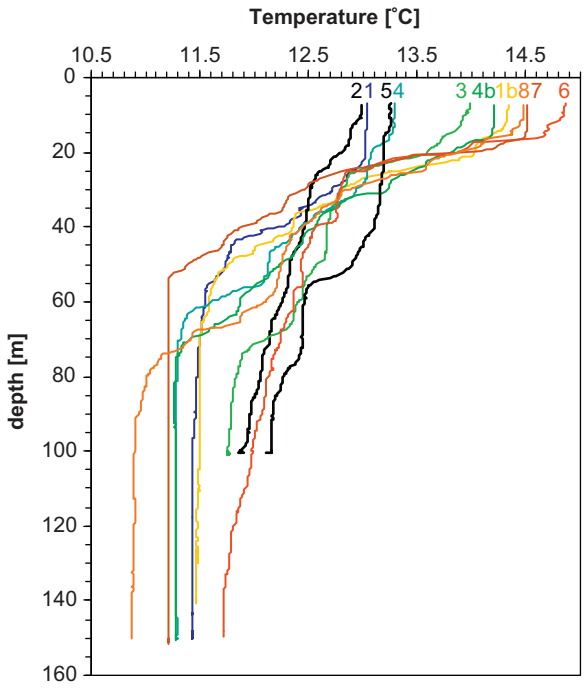


**Fig. 5.** Vertical profiles of temperature (°C) at the different station in northern Bay of Biscay in June 2006. Black profiles correspond to the stations (2 and 5) located on the continental slope.

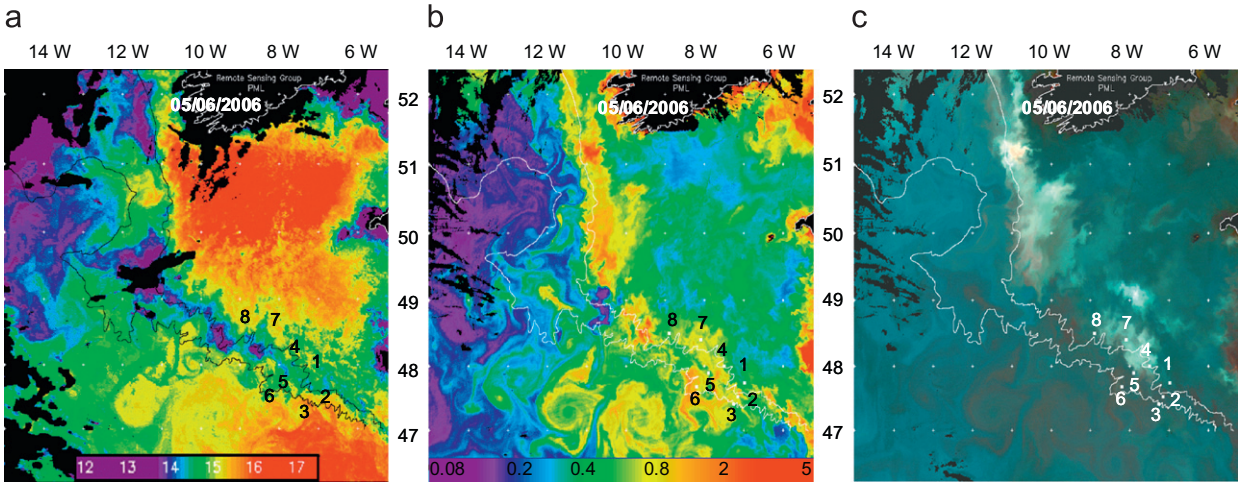


**Fig. 4.** a- Advanced Very High Resolution Radiometer (AVHRR) SST (5th June 2006) b- Moderate-resolution Imaging Spectrometer (MODIS) Chl-a (5th June 2006); c- MODIS false-colour reflectance composite (5th June 2006).

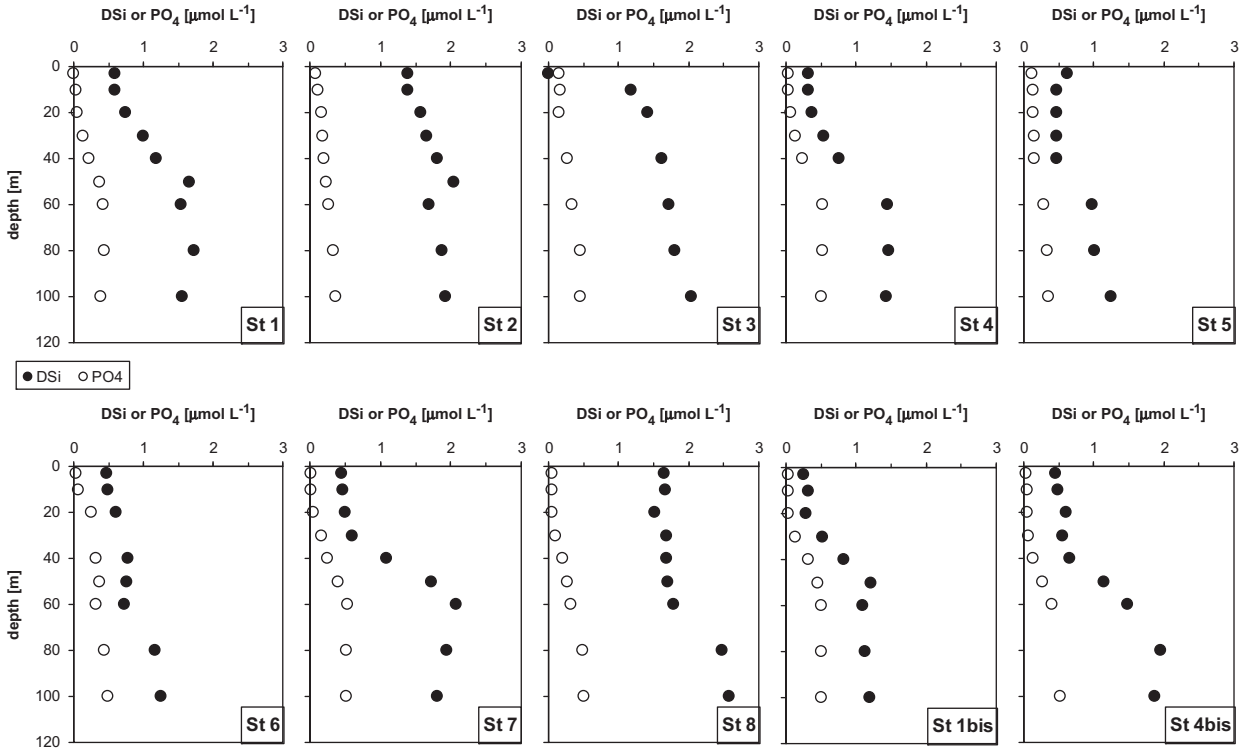


**Fig. 6.** Vertical profiles of $PO_4$ and DSi ($\mu mol\ L^{-1}$) in northern Bay of Biscay in June 2006. Stations 1, 4, 7 and 8 and the revisited stations 1bis and 4bis are located over the continental shelf, stations 2 and 5 are located over the continental slope, and stations 3 and 6 are deeper stations.

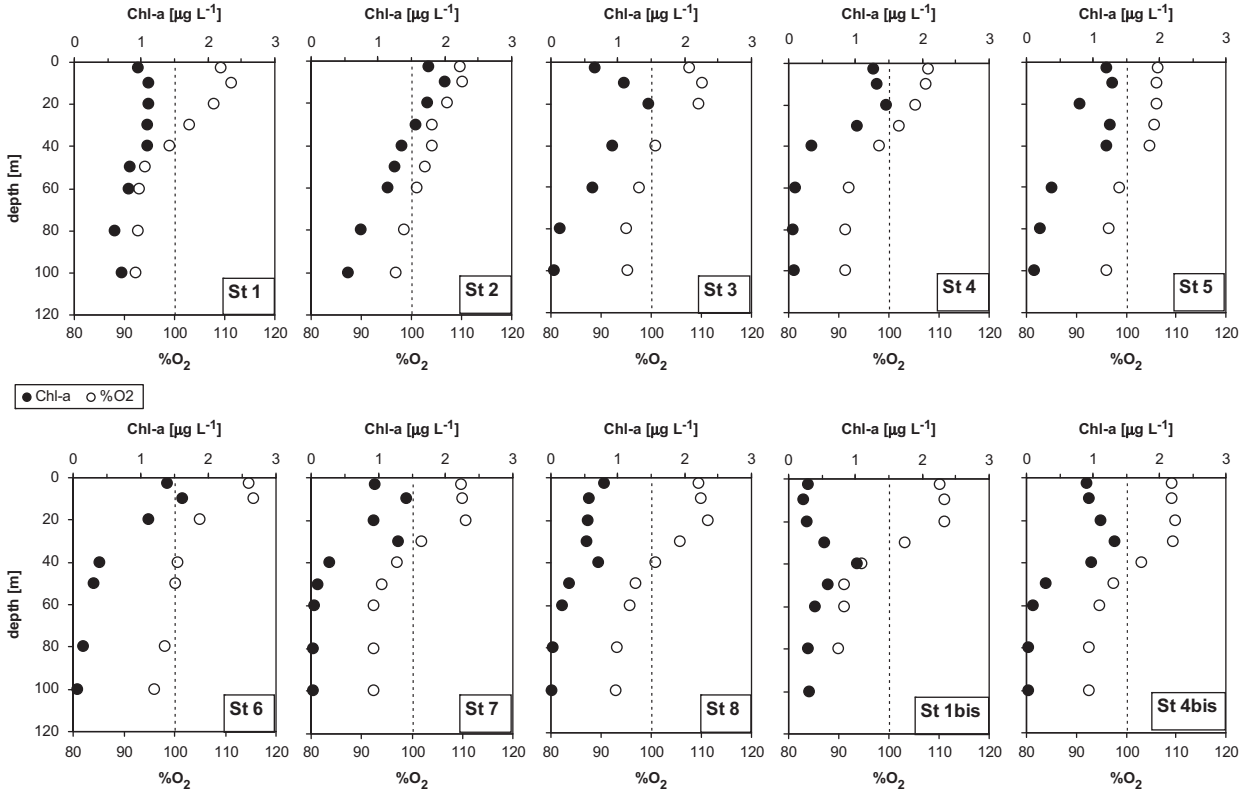


**Fig. 7.** Vertical profiles of Chl-a ($\mu g\ L^{-1}$) and $\%O_2$ (%) in northern Bay of Biscay in June 2006. Stations 1, 4, 7 and 8 and the revisited stations 1bis and 4bis are located over the continental shelf, stations 2 and 5 are located over the continental slope, and stations 3 and 6 are deeper stations.

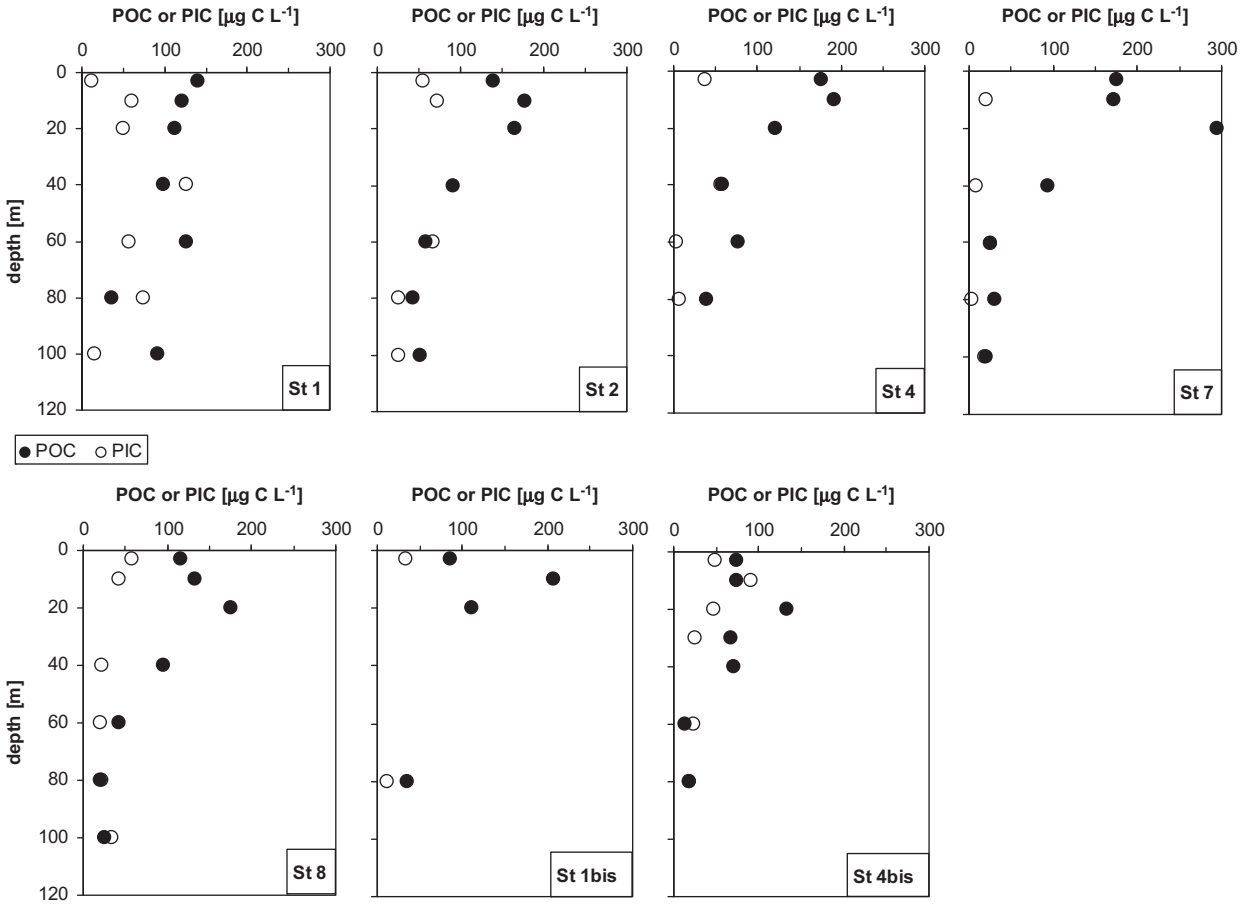


**Fig. 8.** Vertical profiles of POC and PIC concentrations ($\mu g\ C\ L^{-1}$) in northern Bay of Biscay in June 2006. Stations 1, 4, 7 and 8 and the revisited stations 1bis and 4bis are located over the continental shelf, station 2 is located over the continental slope, and stations 3, 5 and 6 were not sampled for this parameter.

and 4bis). The Chl-a concentration reported here was within the range reported by Rees et al. (2002) ($<1.4\ \mu g\ L^{-1}$) and Head et al. (1998) ($<0.8\ \mu g\ L^{-1}$), during early stages of coccolithophore blooms in the North Sea.

Daily depth-integrated PP (Table 2) was globally lower than or close to $1000\ mg\ C\ m^{-2}\ d^{-1}$ except for station 2 (continental slope), where a maximum value of $2160\ mg\ C\ m^{-2}\ d^{-1}$ was observed (Table 2). The lowest PP rate was measured at station 8 ($430\ mg\ C\ m^{-2}\ d^{-1}$), in the HR zone. These PP values were of the same magnitude to those reported in the same area in June 2004 (Harlay et al., 2010).

As a result of biological activity, the UML was oversaturated in $O_2$ with respect to atmospheric equilibrium down to 30–40 m depth (Fig. 7). Oxygen saturation increased up to 110% at the depth of the Chl-a maximum. The underlying waters remained undersaturated in $O_2$ with respect to atmospheric equilibrium, with levels never decreasing below 92%. The POC concentration ranged between 58 and 295 $\mu g\ C\ L^{-1}$ in the top 40 m (at stations 4 and 7, respectively) (Fig. 8). The range of POC values in the photic layer was consistent with those determined during an early coccolithophore bloom in the northern North Sea in June 1994 (200–230 $\mu g\ C\ L^{-1}$; Marañon and González, 1997; Head et al., 1998), and in the northern Bay of Biscay in June 2004 (42–86 $\mu g\ C\ L^{-1}$; Harlay et al., 2010). The highest value (295 $\mu g\ C\ L^{-1}$ at 20 m, station 7) was close to those reported in a decaying bloom off Shetland in July 1993 (336 $\mu g\ C\ L^{-1}$; van der Wal et al., 1995). PIC in the water column ranged between 21 and 127 $\mu g\ C\ L^{-1}$ (Fig. 8) due to the presence of coccolithophores, as supported by HPLC analysis of phytoplankton pigments (see hereafter), scanning electron microscope images (not shown) that identified *E. huxleyi* as the most abundant species, and anomalies of total alkalinity (TA) measured during this cruise and reported by Suykens et al. (2010a). The PIC concentrations were typical for the study area (Harlay et al., 2010) and slightly higher than those reported in the northern North Sea in June 1994 (26–50 $\mu g\ C\ L^{-1}$; Head et al., 1998). The PIC:POC ratio ranged between 0.23 and 0.66, except at station 7 ($\sim$0.10) and in the surface sample at station 1 ($\sim$0.20). Values of the PIC:POC ratio were higher than those reported in the same area (0.20–0.30) in June 2004 (Harlay et al., 2010) and in the North Sea in June 1994 ($<0.25$; Head et al., 1998).

Depth integrated CAL ranged from 90 to $620\ mg\ C\ m^{-2}\ d^{-1}$ at stations 1 and 2, respectively. The lowest CAL values, between 90 and $160\ mg\ C\ m^{-2}\ d^{-1}$ were observed at stations 1, 4 and 8. These values were in agreement with the rates determined in the same area in June 2004 (Harlay et al., 2010). At the revisited station 1bis, CAL increased by $100\ mg\ C\ m^{-2}\ d^{-1}$, and the PP decreased by $240\ mg\ C\ m^{-2}\ d^{-1}$ after 9 days. At the revisited station 4bis CAL decreased by $10\ mg\ C\ m^{-2}\ d^{-1}$ while PP increased by $10\ mg\ C\ m^{-2}\ d^{-1}$ after 6 days.

Values of DCR in sub-surface waters ranged between $-2.2$ and $-5.2\ mmol\ O_2\ m^{-3}\ d^{-1}$ at stations 1 and 8, respectively, and ranged between $-0.1$ and $-2.3\ mmol\ O_2\ m^{-3}\ d^{-1}$ below the photic zone (Fig. 9). At all stations, the vertical pattern of DCR paralleled the distribution of PP (Fig. 10) that exhibited higher values in the photic layer and considerably reduced values below the UML. These DCR values are consistent with those previously reported in surface waters during coccolithophore blooms, ranging from $-2.9$ to $-4.9\ mmol\ O_2\ m^{-3}\ d^{-1}$ in the North Atlantic in

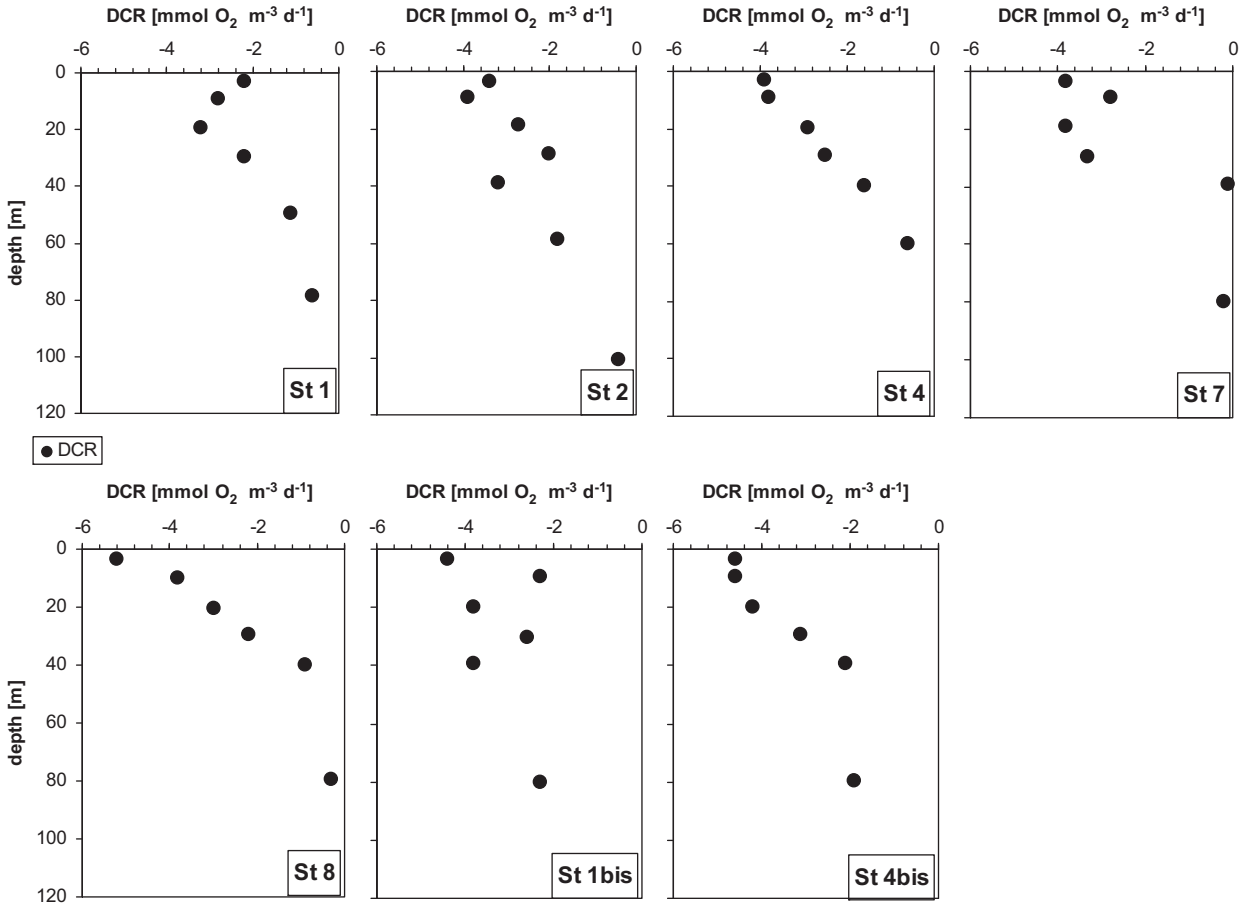


**Fig. 9.** Vertical profiles of DCR (mmol $O_2$ $m^{-3}$ $d^{-1}$) in northern Bay of Biscay in June 2006. Stations 1, 4, 7 and 8 and the revisited stations 1bis and 4bis are located over the continental shelf, station 2 is located over the continental slope, and stations 3, 5 and 6 were not sampled for this parameter.

June 1991 (Holligan et al., 1993) and from −1.8 to −3.7 mmol $O_2$ $m^{-3}$ $d^{-1}$ in the North Sea in June 1999 (Robinson et al., 2002).

The CAL to PP ratio (CAL:PP, Table 2) varied considerably from one station to another, ranging from 0.01 (station 8 at 20 m) to 1.13 (station 4bis at 3 m). The average CAL:PP ratio ($0.29 \pm 0.25$; $n=18$) during our cruise was higher than that reported in the Bay of Biscay in June 2004 (range 0.02–0.31; average 0.16 ($n=11$); Harlay et al., 2010), than in the North Sea in July 1993 (0.03–0.18; van der Wal et al., 1995) and June 1994 (0.14–0.16; Head et al., 1998), and off Iceland in June 1991 (0.14–0.19; Fernández et al., 1993).

## 4. Discussion

Diatoms and coccolithophores are the two major groups having a significant impact on phytoplankton biomass during the spring–summer phytoplankton succession in the Bay of Biscay, but other phytoplankton groups like dinoflagellates, autotrophic prokaryotes (*Prochlorococcus* and *Synechococcus*) and autotrophic picoeukaryotes are also present (Hydes et al., 2001; Sharples et al., 2009). The analysis of the remotely sensed Chl-a shows that our cruise was after the main spring phytoplankton bloom in mid-April (Fig. 3) that is typically dominated by diatoms (Hydes et al., 2001; Joint et al., 2001). This is corroborated by the analysis of the distribution of biogeochemical variables showing very low DSi and $PO_4$ concentrations in surface waters, low Chl-a values, $O_2$ over-saturation and $CO_2$ under-saturation with respect to atmospheric equilibrium (Section 3.2, Table 2). The low DSi concentrations in the photic zone (Fig. 6) may have disadvantaged diatoms against coccolithophores (Egge and Aksnes, 1992; Egge and Heimdal, 1994; Lessard et al., 2005) that in addition can rely on dissolved organic phosphorus to meet their phosphorous requirements (Riegman et al., 2000). The remotely sensed SST (Fig. 4) and vertical profiles of temperature (Fig. 5), suggest enhanced vertical mixing at the continental slope, associated nearby with relatively higher Chl-a values and HR. We hypothesize that mixing at continental slope allowed the injection of inorganic nutrients that triggered the blooming of mixed phytoplankton communities dominated by coccolithophores. Since the sampled stations were distributed along a spatial gradient from cool (low stratification) to warm (higher stratification) waters, we use hereafter an indicator of stratification ($\Delta\rho_{100\ \mathrm{m-3\ m}}$) to classify the different sampled stations, and to reconstruct the possible evolution of the bloom from the onset at the continental slope (triggered by vertical mixing) through its development as the water mass was advected on-shelf and stratified.

### 4.1. Biogeochemical features due to the bloom development as determined by the degree of water column stratification

Stratification is one of the most important variables controlling PP and the succession of phytoplankton communities (e.g., Margalef, 1997). The increase of stratification leads to the decrease of vertical inputs of inorganic nutrients (Rost and Riebesell, 2004) and DIC (Borges et al., 2008) but enhances light conditions for phytoplankton development. Such environmental changes drive a succession of phytoplankton communities from diatoms to coccolithophores that exhibit higher tolerance for high light

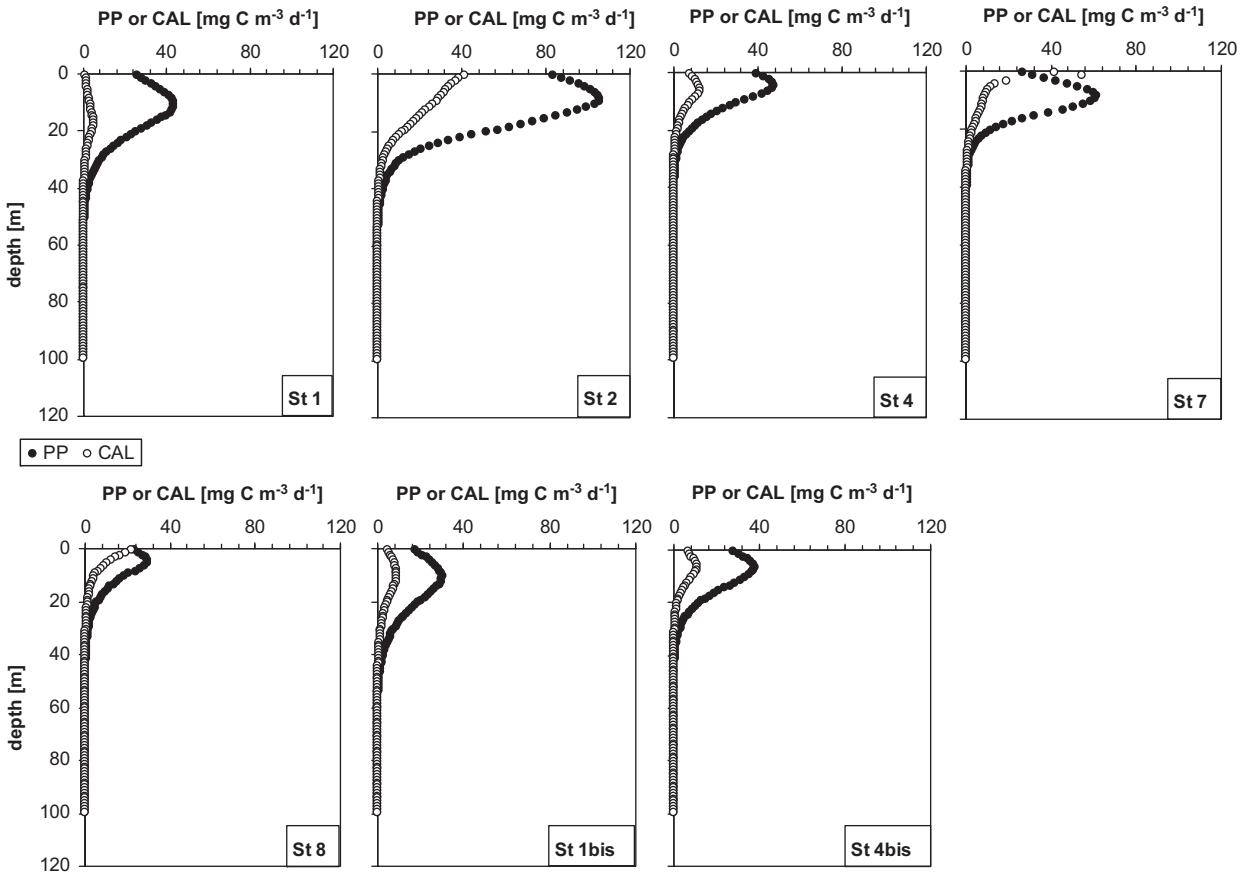


**Fig. 10.** Vertical profiles of PP and CAL (mg C $m^{-3}$ $d^{-1}$) computed from PPvsPAR and CALvsPAR, respectively in northern Bay of Biscay in June 2006. Stations 1, 4, 7 and 8 and the revisited stations 1bis and 4bis are located over the continental shelf, station 2 is located over the continental slope, and stations 3, 5 and 6 were not sampled for this parameter.

(Balch et al., 1992; Nanninga and Tyrrell, 1996) and are associated with lower $pCO_2$ (Dong et al., 1993; Brownlee et al., 1994; Nimer et al., 1994). They are able to outcompete diatoms under low inorganic nutrient concentrations, and/or deviating from the Redfield stoichiometry. We attempted reconstructing the bloom sequence and succession of the mixed phytoplankton community and the ecological niche favourable for coccolithophores, by plotting biogeochemical parameters and processes against $\Delta\rho_{100\ m-3\ m}$ (Figs. 11–13).

The $PO_4$ concentrations in surface waters significantly decreased with increase in stratification whereas no clear trend was apparent for DSi in surface water that remained below 2.0 μmol $L^{-1}$ (Fig. 11). The decrease of $PO_4$ availability could explain the decrease of integrated Chl-a, indicative of the bloom ageing and in decline. With increasing stratification, PP decreased while CAL increased for stations over the shelf (Fig. 13).

The phytoplankton community was dominated by coccolithophores (Prymnesiophytes), representing about 42% of total Chl-a at the onset of the bloom (station 2, low stratification), and decreased with stratification (Fig. 11). The contribution of diatoms to total Chl-a was highly variable, ranging from 5% (station 8) to 44% (stations 7 and 4bis) and did not show any significant pattern with increasing stratification, but an increase with decrease in DSi concentrations. The low values of DSi (below 2.0 μM) are likely to limit growth of large heavily silicified diatoms (Paasche, 1973; Egge and Aksnes, 1992). Microscopic observations showed a dominance, in terms of biovolume, of large and lightly silicified diatoms (*Rhizosolenia spp.*) which can explain the high abundances (~44%) at the stations 4bis and 7 with a high degree of stratification (N. Van Oostende and K. Sabbe, unpublished results, 2010). The increase with stratification of phototrophic dinoflagellate biomass and of other groups (chrysophytes, prasinophytes, cryptophytes and cyanobacteria) is characteristic of coccolithophore bloom decline, and has also been observed in mesocosms (Riebesell et al., 2007).

A significant decrease of transparent exopolymer particles (TEP−$C_{micro}$ as reported for this cruise by Harlay et al., 2009) was observed with increasing stratification and nutrient depletion (Fig. 12). No clear pattern was observed in the POC concentration with increasing stratification, while PIC decreased, leading to a decrease in the PIC:POC ratio (Fig. 12). However, PP decreased and CAL increased with stratification, leading to a significant increase of the CAL:PP ratio ($r^2$=0.79) (Fig. 13). This suggests a decoupling between standing stocks of POC and PIC and their respective production rates, favouring export of biogenic material to depth. Stations located in the HR patch (4, 4bis, 7 and 8) showed low PIC compared to those at stations 1 and 2, located outside the HR patch. Indeed, the optical properties of this HR patch were due to abundant shed liths in surface waters (e.g., Holligan et al., 1993) and were not necessarily associated with high PIC concentrations. The increase of CAL (and CAL:PP ratio) for stations over the shelf (excluding stations 2 and 5) is characteristic of coccolithophore bloom development from high-PP and low-CAL during the early bloom phase to low-PP and high-CAL during stationary and declining bloom phases (Fig. 13). Such a change was accompanied by an increase of heterotrophic processes, as featured by the increase of DCR with stratification, although there was no pattern of BP with stratification (Fig. 13).

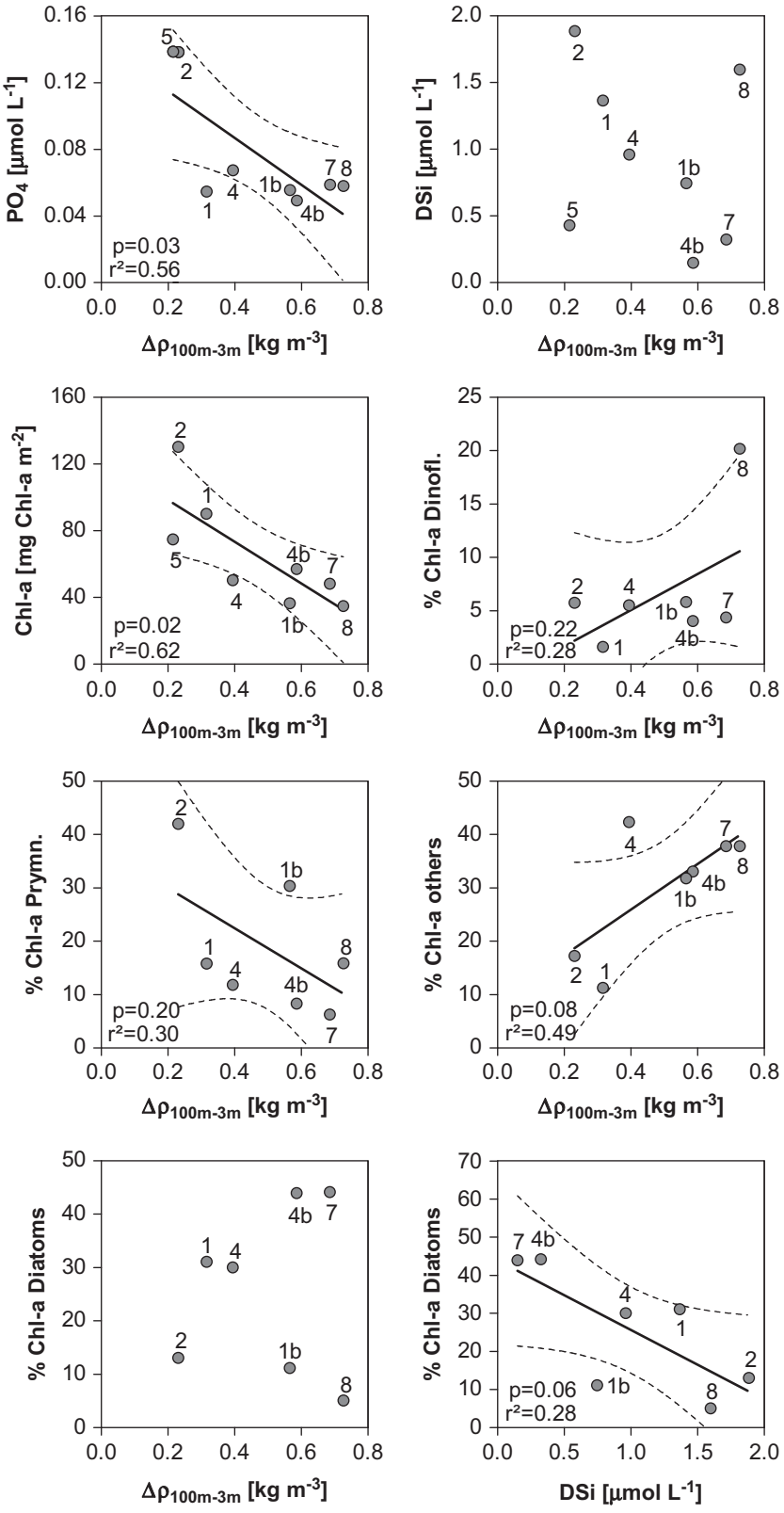


**Fig. 11.** Depth averaged $PO_4$ (µmol $L^{-1}$) and DSi (µmol $L^{-1}$) in the 30 m top layer, depth integrated Chl-a (mg Chl-a $m^{-2}$) in the photic zone and the relative percentage of Chl-a for Dinoflagellates (% Chl-a Dinofl.), Prymnesiophytes (% Chl-a prym.), other phytoplankton groups (% Chl-a Others) and diatoms (% Chl-a Diatoms), (integrated over the top 30 m) *versus* the difference of density at 3 m depth and at 100 m depth ($\Delta\rho_{100\ m-3\ m}$) in northern Bay of Biscay in June 2006. The linear regression and the 95% confidence intervals (dashed lines) are represented together with the determination coefficient ($r^2$). Plain regression lines are based on all stations, dashed regression lines are based on the continental shelf stations (excluding the continental slope—stations 2 and 5). Numbers refer to the sampling station.

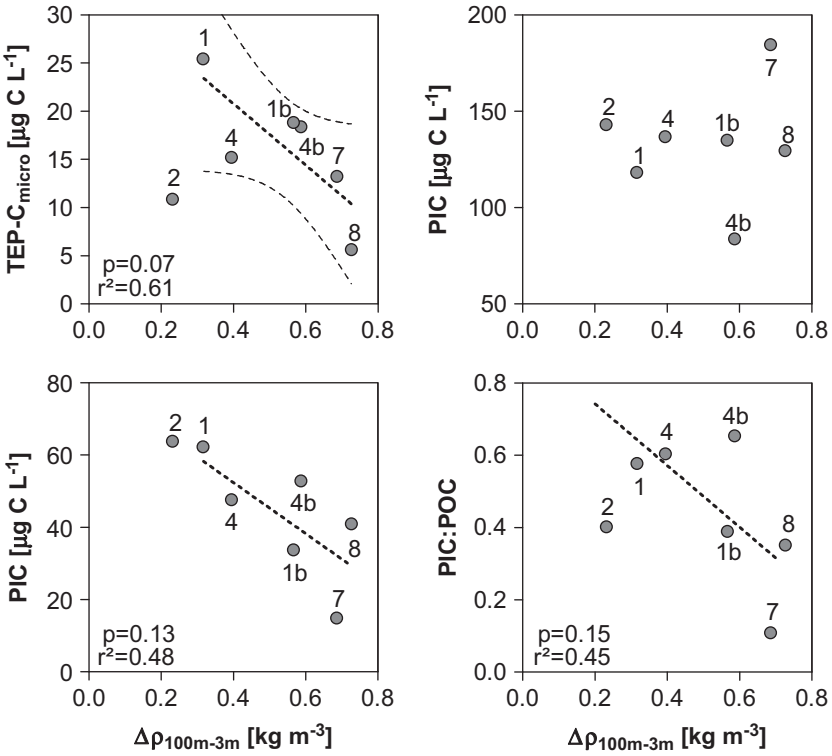


**Fig. 12.** Depth averaged TEP-$C_{micro}$ (µg C $L^{-1}$, from Harlay et al., 2009), POC (µg $L^{-1}$), PIC (µg $L^{-1}$) and PIC:POC ratio in the top 30 m *versus* the difference of density at 3 m depth and at 100 m depth ($\Delta\rho_{100\ m-3\ m}$) in northern Bay of Biscay in June 2006. The linear regression and the 95% confidence intervals (dashed lines) are represented together with the determination coefficient ($r^2$). Plain regression lines are based on all stations, dashed regression lines are based on the continental shelf stations (excluding the continental slope—stations 2 and 5). Numbers refer to the sampling station.

### 4.2. Trophic status of the coccolithophore bloom

A community is termed "autotrophic" when gross primary production (GPP) is higher than community respiration and "heterotrophic" when community respiration exceeds GPP (e.g., Gattuso et al., 1998). However, the trophic status of a community does not necessarily imply that it is a source or a sink for atmospheric $CO_2$, since the direction of the air–sea $CO_2$ fluxes results from a combination of several biogeochemical and physical processes acting at different time scales (e.g., Borges et al., 2006). The $pCO_2$ values in surface waters during the cruise ranged from 265 to 353 µatm and indicate that the area was undersaturated with respect to atmospheric equilibrium (~376 µatm) (Table 2), acting as a sink for atmospheric $CO_2$ ranging between −8.5 and −17.8 mmol C $m^{-2}$ $d^{-1}$ (Table 3; Suykens et al., 2010a). The range of $pCO_2$ values was comparable to those reported during coccolithophore blooms in the Bering Sea (Murata and Takizawa, 2002), the North Sea (Buitenhuis et al., 1996) and the northern North Atlantic (Robertson et al., 1994), and in the Bay of Biscay in June 2004 (Harlay et al., 2010).

Based on the measurement of metabolic rates, the trophic status of the coccolithophore bloom was assessed, considering that the $^{14}C$-based rate measurement of PP reflected GPP, based on the short duration of the incubations (Gazeau et al., 2007). The community evolved from net autotrophy at the early stage of the bloom, station 2 (PP:DCR=2.2), to net heterotrophy at station 8 (PP:DCR=0.3) when PP rates decreased (Fig. 14). The same pattern of decreasing PP:DCR with decrease in PP was also reported during a coccolithophore bloom in the North Sea in June 1999 (based on $O_2$ incubations for both PP and DCR, Robinson et al., 2002). The PP:DCR ratio was on average 0.73 ± 0.47 ($n$=7), similar to the values reported in the North Sea in June 1999 ranging from 0.18 to 1.29, on average 0.89 ± 0.37 ($n$=8, Robinson et al., 2002).

### 4.3. Carbon mass balance in the photic zone

The C cycle in the photic zone is driven by GPP and community respiration, the balance of these two terms corresponds to the net community production (NCP). In coccolithophore blooms, CAL is an additional source of $CO_2$ to the surrounding seawater that modulates the net balance of community $CO_2$ fluxes (Purdie and Finch, 1994; Crawford and Purdie, 1997; Frankignoulle and Borges, 2001; Suykens et al., 2010a). The NCP, corresponding to the potential for C export from the photic layer to the aphotic zone, was compared to the integrated $DCR_{aphotic}$ in the aphotic layer (i.e., the aphotic C demand). NCP was calculated in the photic layer as:

$$NCP = PP - DCR_{photic},$$

where PP and DCR are expressed as $CO_2$ fluxes.

The net metabolic $CO_2$ flux (NMCF) was compared to the air–sea $CO_2$ flux computed from $pCO_2$ measurements and was calculated as:

$$NMCF = NCP + 0.6CAL$$

where 0.6CAL is the flux of $CO_2$ released to the water column by CAL (Frankignoulle et al., 1994).

The early bloom phase (stations 2 and 1) was characterized by high PP and CAL values (Table 2). The NMCF (−67.9 mmol C $m^{-2}$ $d^{-1}$ at station 2) had the same direction as the air–sea $CO_2$ flux (−11.4 mmol C $m^{-2}$ $d^{-1}$). At station 2, the NCP was positive, indicating a net autotrophic status leading to a positive potential C export (+98.7 mmol C $m^{-2}$ $d^{-1}$) that was of the same order of magnitude as the aphotic pelagic C demand (89.0 mmol C $m^{-2}$ $d^{-1}$).

At the stations representative of more developed and declining bloom conditions (stations 4, 4bis, 7 and 8), PP and CAL were lower than the early bloom phase (stations 2 and 5), and NCP was neutral or negative, indicating a balanced or a net heterotrophic status (ranging from +5.5 to −68.8 mmol C $m^{-2}$ $d^{-1}$). At these stations,

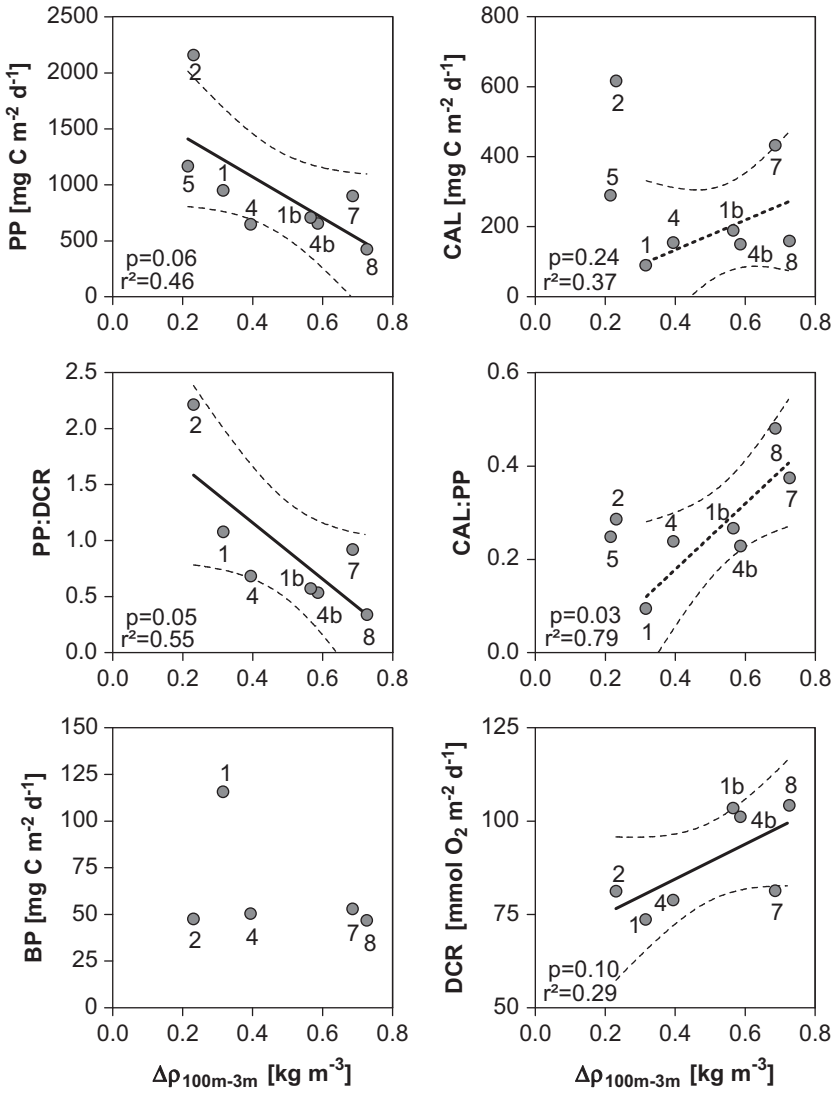


**Fig. 13.** PP (mg C $m^{-2}$ $d^{-1}$), CAL (mg C $m^{-2}$ $d^{-1}$), PP:DCR ratio, CAL:PP ratio, BP (mg C $m^{-2}$ $d^{-1}$) and DCR (mmol $O_2$ $m^{-2}$ $d^{-1}$) *versus* the difference of density at 3 m depth and at 100 m depth ($\Delta\rho_{100\ m-3\ m}$) in northern Bay of Biscay in June 2006. The linear regression and the 95% confidence interval (dashed lines) are represented together with the determination coefficient ($r^2$). Plain regression lines are based on all stations, dashed regression lines are based on the continental shelf stations (excluding the continental slope—stations 2 and 5). Numbers refer to the sampling station.

**Table 3**
Carbon fluxes (mmol C $m^{-2}$ $d^{-1}$) in the northern Bay of Biscay in June 2006 based on a mass related to fixation of $CO_2$ by PP (the particulate gross primary production), to release of $CO_2$ by CAL (using an average molar ratio of $CO_2$ production to $CaCO_3$ production of 0.6, Frankignoulle et al. (1994), hence, 0.6 × CAL), and to the release of $CO_2$ by DCR (integrated in the photic layer and converted to C units using a respiratory quotient of 1). The net metabolic $CO_2$ flux corresponds to the net balance of $CO_2$ fixed by PP and $CO_2$ release by CAL and DCR. Net air–sea $CO_2$ flux was computed from measurements of $pCO_2$ (as detailed by Suykens et al. 2010a). Export of organic C corresponds to the net balance of PP and DCR (integrated in the photic layer). Aphotic C demand corresponds to DCR integrated in the aphotic layer (to the sea floor depth except for station 2 (total depth of 680 m) where integration was carried out to the depth of deepest sample (100 m)). Stations were classified from the less to most stratified conditions.

| Station | $CO_2$ fluxes (mmol C $m^{-2}$ $d^{-1}$) | | | | | C fluxes (mmol C $m^{-2}$ $d^{-1}$) | |
|---|---|---|---|---|---|---|---|
| | Related to PP | Related to CAL | Related to DCR | Net metabolic $CO_2$ flux | Net air–sea $CO_2$ flux | Export of organic C | Aphotic C demand |
| 2 | −180.0 | 30.9 | 81.3 | −67.9 | −11.4 | 98.7 | 89.0 |
| 1 | −79.3 | 4.5 | 73.7 | −1.0 | −−17.8 | 5.5 | 98.2 |
| 4(HR) | −54.0 | 7.8 | 78.9 | 32.6 | −13.4 | −24.9 | 66.9 |
| 1bis | −59.2 | 9.5 | 103.5 | 53.8 | −16.1 | −44.4 | 159.0 |
| 4bis(HR) | −54.6 | 7.5 | 101.2 | 54.1 | −10.7 | −46.6 | 168.5 |
| 7(HR) | −75.1 | 21.7 | 81.4 | 28.0 | −10.2 | −6.4 | 35.1 |
| 8(HR) | −35.5 | 8.0 | 104.3 | 76.8 | −8.5 | −68.8 | 72.3 |

the NMCF was positive (+32.6 and +76.8 mmol $CO_2$ $m^{-2}$ $d^{-1}$) while the air–sea $CO_2$ flux remained negative (−8.5 and −17.8 mmol $CO_2$ $m^{-2}$ $d^{-1}$). The potential C export was negative (−24.9 to −68.8 mmol C $m^{-2}$ $d^{-1}$); hence, insufficient to sustain either the aphotic pelagic C demand (between 35.1 and 168.5 mmol C $m^{-2}$ $d^{-1}$) or the benthic respiration, ranging during

the cruise from −2.3 to −7.2 mmol $O_2$ $m^{-2}$ $d^{-1}$ at stations 2, 4, 4bis and 8 (Suykens et al., 2010b).

One caveat in the community C mass balance given in Table 3 is that a steady state was assumed. It is well established that in aquatic ecosystems there is a variable but usually strong decoupling in time and space of organic C production and consumption. This decoupling could explain the low export of organic carbon computed at most stations that cannot meet the aphotic C demand. Furthermore, air–sea $CO_2$ fluxes are an integrated signal of the water mass biogeochemical history because of the very long equilibration time of surface waters with respect to atmospheric $CO_2$ due to the buffering capacity of seawater. Also, $CO_2$ dynamics integrate both physical (e.g., vertical mixing, advection, and water residence time) and purely thermodynamic (mainly water temperature change) effects, as discussed at length by e.g., Borges et al. (2006). This appears to be the most likely explanation for the net sink of atmospheric $CO_2$ computed from the $pCO_2$ measurements for all stations, while the balance of community metabolic rates leads to a net release of $CO_2$ in the photic layer during the maturing and declining bloom phases.

The other caveat in the C mass balance (Table 3) is that we only considered the measurements of PP in the particulate phase. In all aquatic ecosystems, the contribution of dissolved PP ($PP_d$) is variable but always significant compared to particulate PP (e.g., Baines and Pace, 1991). We did not measure $PP_d$ due to the difficulty of estimating this quantity with the $^{14}C$ incubation method (Marra, 2002 and references therein). The biogeochemical model of Joassin et al. (2008) that describes C dynamics in coccolithophore blooms validated with mesocosm experiments (Delille et al., 2005), was used to estimate $PP_d$ and to refine the C mass balance (Table 4). Estimated $PP_d$ ranged between 14% and 28% of total primary production ($PP_{tot}$ = PP + $PP_d$) which is similar to the range (6–24%) reported by Rees et al. (2002) during a coccolithophore bloom in the North Sea in June 1999.

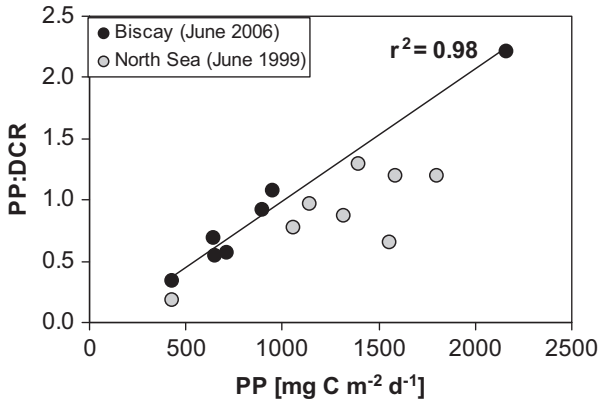


**Fig. 14.** PP:DCR *versus* PP (mg C $m^{-2}$ $d^{-1}$) in northern Bay of Biscay in June 2006 and in the North Sea in June 1999, during a coccolithophore bloom (Robinson et al., 2002).

Based on the C mass balance accounting for $PP_d$ (Table 4), NMCF was negative at stations 1, 2, 4 and 5, at rates of the same order of magnitude as the air–sea $CO_2$ fluxes. The NMCF was balanced at station 7. At stations 1, 2, 4, 5 and 7, a net export of organic C was computed that is of the same order of magnitude as the aphotic C demand. The trend in export of organic C is consistent with the conceptual model of bloom development with higher C export at the onset of the bloom (stations 1, 2 and 5), lower C export at the mature bloom phase (stations 4 and 7), and low or no export during the declining bloom phase (stations 8, 1bis and 4bis). This is also consistent with the phytoplankton composition derived from HPLC measurements showing an increasing contribution of dinoflagellates, chrysophytes, prasinophytes and cryptophytes as the bloom matured and declined (Fig. 11), since most of these phytoplankton species have a low potential for sedimentation and vertical export due to their small size, lack of inorganic cell wall structures, or mobility (flagellates).

Labile sugars are high C content organic compounds exuded by phytoplankton, constituting a fraction of the C released by $PP_d$. Their contribution to the C fixed photosynthetically, depends on the growth stage of the coccolithophore *E. huxleyi* (Fernández et al., 1996). Among dissolved C losses, of particular interest is the production of some polysaccharides that can aggregate to form sticky C-rich particles such as TEP (Passow, 2002). During mesocosm experiments with *E. huxleyi*, C losses due to TEP formation and settling of aggregates had a significant impact on the C budget (Engel et al., 2004; Delille et al., 2005; Joassin et al., 2008). During this cruise, the carbon content of TEP (TEP-C) averaged 12% of POC and attained 68% of POC at certain depths (Harlay et al., 2009). The dynamics of TEP formation during bloom development modifies the properties of macroaggregates (Logan et al., 1995; Engel, 2000; Kahl et al., 2008) and the presence of calcite in these aggregates increases their settling velocity (ballast effect; François et al., 2002). However, TEP concentrations were higher during the early phases of the bloom and tightly coupled to primary production and phytoplankton standing stocks (Fig. 12). This is consistent with the low export of C computed for the maturing and declining bloom phases (Tables 3 and 4). The comparison of the C mass balances given in Tables 3 and 4, certainly highlights the importance of $PP_d$ in C flows during coccolithophore blooms, although it is acknowledged that the estimates of $PP_d$ herein are rough approximations and should be used with caution.

## 5. Synthesis and conclusions

A bloom of mixed phytoplankton community dominated by coccolithophores was studied at the continental margin of the northern Bay of Biscay, where enhanced biological activity resulted

**Table 4**
Carbon fluxes (mmol C $m^{-2}$ $d^{-1}$) in the northern Bay of Biscay in June 2006. All computations are identical to Table 2 (refer to caption for details) with the exception that $PP_{tot}$ corresponds to the sum of particulate PP and $PP_d$ (computed using the biogeochemical model of Joassin et al., 2008).

| Station | $CO_2$ fluxes (mmol C $m^{-2}$ $d^{-1}$) | | | | | C fluxes (mmol C $m^{-2}$ $d^{-1}$) | |
|---|---|---|---|---|---|---|---|
| | Related to $PP_{tot}$ | Related to CAL | Related to DCR | Net metabolic $CO_2$ flux | Net air–sea $CO_2$ flux | Export of organic C | Aphotic C demand |
| 2 | −205.6 | 30.9 | 81.3 | −93.5 | −11.4 | 124.3 | 89.0 |
| 1 | −108.8 | 4.5 | 73.7 | −30.5 | −17.8 | 35.0 | 98.2 |
| 4(HR) | −114.4 | 7.8 | 78.9 | −27.8 | −13.4 | 35.5 | 66.9 |
| 1bis | −65.7 | 9.5 | 103.5 | 47.3 | −16.1 | −37.9 | 159.0 |
| 4bis(HR) | −63.8 | 7.5 | 101.2 | 44.9 | −10.7 | −37.4 | 168.5 |
| 7(HR) | −101.4 | 21.7 | 81.4 | 1.7 | −10.2 | 19.9 | 35.1 |
| 8(HR) | −39.2 | 8.0 | 104.3 | 73.1 | −8.5 | −65.1 | 72.3 |

from local nutrient inputs into the UML, due to physical forcing (mainly internal tides) as deduced from vertical profiles of temperature and remotely sensed SST (cooler and less stratified water patches at the shelf break and the continental slope). It is hypothesized that the vertical mixing at the shelf-break triggered the bloom of mixed phytoplankton communities dominated by coccolithophores, and that the bloom developed and then declined as these water masses were transported over the continental shelf due to baroclinic eddy activity along the edges of the cold water patch, stratifying as they warmed.

The cruise took place after the main spring bloom of, probably, large diatoms that peaked in mid-April (based on the temporal evolution of Chl-a from remote sensing images and modelled deep UML favourable to the development of large diatoms). Hence, during our cruise, the area was strongly depleted in DSi with levels $< 2.0$ μM that are limiting for diatom growth (Egge and Aksnes, 1992). Additional inputs of nutrients by vertical mixing at the shelf break would then favour phytoplankton development and the succession from diatoms to coccolithophores.

The analysis of data as a function of an indicator of stratification allowed the reconstruction of the bloom sequence, whereby coccolithophores dominated in low stratified conditions and, as stratification intensified, their abundance declined in favour of dinoflagellates, chrysophytes, prasinophytes and cryptophytes. Furthermore, coccolithophores shifted from an organic production dominated-phase to a more inorganic production dominated-phase, as shown by the increase of the CAL:PP ratio with stratification.

A C mass balance in the photic layer was computed along a gradient between the high production zone (stations 2 and 5) and the HR zone (station 8). The $pCO_2$ measurements indicated that surface waters acted as a net sink for atmospheric $CO_2$ during all phases of the bloom, although TA data reported by Suykens et al. (2010a) showed that CAL had a large impact on surface seawater dissolved carbonate chemistry. Hence, CAL related to coccolithophore blooms had the potential to decrease the sink of atmospheric $CO_2$ but did not reverse the direction of the flux. Net community autotrophy was only found for the early phase of the bloom. During the maturing and declining phases of the bloom, potential export from the photic layer could not meet the aphotic C demand. This C mass balancing approach suffers from several caveats. Firstly, steady-state is assumed but C dynamics need to be integrated over longer time scales due to the decoupling in time and space of organic carbon production and degradation. Secondly, the importance of $PP_d$ and its potential incorporation into TEP during coccolithophore blooms is likely a significant C flux sustaining the heterotrophic C demand in the twilight zone, as suggested by Koeve (2005). Indeed, when comparing the C mass balance in the photic layer and the air–sea $CO_2$ fluxes and the aphotic C demand, the C community mass balance established using estimated $PP_d$ was more consistent.

The effects of ocean acidification on marine communities will likely lead to a decoupling of C and N cycling, modifying C export to depth and providing a feedback on increasing atmospheric $CO_2$ (Riebesell et al., 2007). As a result of the expected reduction of CAL in bloom forming coccolithophores in a high $CO_2$ ocean (Riebesell et al., 2000; Delille et al., 2005) and associated changes in the ballast of aggregates by biogenic calcite (De La Rocha and Passow, 2007; Hofmann and Schellnhuber, 2009), the biogenic C pumping efficiency of these blooms is likely to be modified in the coming decades and centuries. The magnitude and direction of these changes remain to be established. Comprehensive and multi-disciplinary studies of C cycling in coccolithophore blooms in natural conditions such as the one reported here is an essential prerequisite for a robust and credible implementation in mathematical models to allow the projection of a plausible future evolution of carbon biogeochemistry under global change, in particular in relation to ocean acidification.

## Acknowledgements

The authors are grateful to the officers and crewmembers of the *RV Belgica* for logistic support during the cruise, Joan Backers, Jean-Pierre De Blauw and Gregory Deschepper of the Unit of the North Sea Mathematical Models for support in data acquisition during the cruise, to Pascal Joassin for help in the computations of dissolved primary production, Tim Smyth, Peter Miller, NERC Earth Observation Data Acquisition and Analysis Service for the AVHRR and MODIS images, Nathalie Roevros and Marc-Vincent Commarieu for laboratory analysis, and to Christiane Lancelot, John Huthnance, Jonathan Sharples, Michael Bacon (Associate Editor), and two anonymous reviewers for constructive comments during the elaboration of the manuscript. This study was financed by the Belgian Federal Science Policy Office in the framework of the PEACE project (contract no. SD/CS/03A/B) and by the Helmholtz Association (contract no. HZ-NG-102). This work is a contribution to the EU FP6 European Network of Excellence EUR–OCEANS (contract no. 511106-2), EU IP CARBOOCEAN (contract no. 511176), and SOLAS. CDB was supported by a PhD grant from the EU FP6 IP CarboOcean project (contract no. 511176–2), NVO was supported by a PhD grant from the Institute for the Promotion of Innovation through Science and Technology in Flanders (IWT-Vlaanderen), AVB and BD are research associates at the F.R.S.-F.N.R.S. First and last authors equally contributed to data interpretation and manuscript drafting.

## References

Baines, S.B., Pace, M.L., 1991. The production of dissolved organic matter by phytoplankton and its importance to bacteria: patterns across marine and freshwater systems. Limnology and Oceanography 36, 1078–1090.

Balch, W.M., Holligan, P.M., Kilpatrick, K.A., 1992. Calcification, photosynthesis and growth of the bloom-forming coccolithophore, *Emiliania huxleyi*. Continental Shelf Research 12, 1353–1374.

Balch, W.M., Gordon, H.R., Bowler, B.C., Drapeau, D.T., Booth, E.S., 2005. Calcium carbonate measurements in the surface global ocean based on moderate-resolution imaging spectroradiometer data. Journal of Geophysical Research 110, 1–22.

Balch, W.M., Drapeau, D., Bowler, B., Booth, E., 2007. Prediction of pelagic calcification rates using satellite measurements. Deep Sea Research Part II 54, 478–495.

Balch, W.M., Utgoff, P.E., 2009. Potential interactions among ocean acidification, coccolithophores, and the optical properties of seawater. Oceanography 22, 146–159.

Benson, B.B., Krause, D., 1984. The concentration and isotopic fractionation of oxygen dissolved in freshwater and seawater in equilibrium with the atmosphere. Limnology and Oceanography 29, 620–632.

Billard, C., Inouye, I., 2004. What's new in Coccolithophore Biology?. In: Thierstei, H.R., Youn, J.R. (Eds.), Coccolithophores: From Molecular Processes to Global Impact, pp. 11–30.

Borges, A.V., Schiettecatte, L.-S., Abril, G., Delille, B., Gazeau, F., 2006. Carbon dioxide in European coastal waters. Estuarine, Coastal and Shelf Science 70, 375–387.

Borges, A.V., Tilbrook, B., Metzl, N., Lenton, A., Delille, B., 2008. Inter-annual variability of the carbon dioxide oceanic sink south of Tasmania. Biogeosciences 5, 144–155.

Brownlee, C., Nimer, N.A., Dong, L.F., Merrett, M.J., 1994. Cellular regulation during calcification in *Emiliania huxleyi*. In: Green, J.C., Leadbeater, B.S.C. (Eds.), The Haptophyte Algae. Clarendon Press, Oxford, pp. 133–148.

Buitenhuis, E.T., van Bleijswijk, J.D.L., Bakker, D.C.E., Veldhuis, M.J.W., 1996. Trends in inorganic and organic carbon in a bloom of *Emiliania huxleyi* in the North Sea. Marine Ecology Progress Series 143, 271–282.

Buitenhuis, E.T., van der Wal, P., de Baar, H.J.W., 2001. Blooms of *Emiliania huxleyi* are sinks of atmospheric carbon dioxide: A field and mesocosm study derived simulation. Global Biogeochemical Cycles 15, 577–587.

Crawford, D.W., Purdie, D.A., 1997. Increase of $pCO_2$ during blooms of *Emiliania huxleyi*: Theoretical considerations on the asymmetry between acquisition of $HCO_3^-$ and respiration of free $CO_2$. Limnology and Oceanography 42, 365–372.

De Bodt, C., Harlay, J., Chou, L., 2008. Biocalcification by *Emiliania huxleyi* in batch culture experiments. Mineralogical Magazine 72, 251–256.

De Bodt, C., Van Oostende, N., Harlay, J., Sabbe, K., Chou, L., 2010. Individual and interacting effects of $pCO_2$ and temperature on *Emiliania huxleyi* calcification:

study of the calcite production, the coccolith morphology and the coccosphere size. Biogeosciences 7, 1401–1412.
De La Rocha, C.L., Passow, U., 2007. Factors influencing the sinking of POC and the efficiency of the biological carbon pump. Deep Sea Research Part II 54, 639–658.
Delille, B., Harlay, J., Zondervan, I., Jacquet, S., Chou, L., Wollast, R., Bellerby, R.G.J., Frankignoulle, M., Borges, A.V., Riebesell, U., Gattuso, J.-P., 2005. Response of primary production and calcification to changes of $pCO_2$ during experimental blooms of the coccolithophorid *Emiliania huxleyi*. Global Biogeochemical Cycles 19, GB2023.
Dong, L.F., Nimer, N.A., Okus, E., Merrett, M.J., 1993. Dissolved inorganic carbon utilization in relation to calcite production in *Emiliania huxleyi* (Lohmann) Kamptner. New Phytologist 123, 679–684.
Egge, J.K., Aksnes, D.L., 1992. Silica as regulating nutrient in phytoplankton competition. Marine Ecology Progress Series 83, 281–289.
Egge, J.K., Heimdal, B.R., 1994. Blooms of *Emiliania huxleyi* in mesocosm experiment; effects of nutrient supply in different N:P ratios. Sarsia 79, 333–348.
Engel, A., 2000. The role of transparent exopolymer particles (TEP) in the increase in apparent particle stickiness (alpha) during the decline of a diatom bloom. Journal of Plankton Research 22, 485–497.
Engel, A., Thoms, S., Riebesell, U., Rochelle-Newall, E., Zondervan, I., 2004. Polysaccharide aggregation as a potential sink of marine dissolved organic carbon. Nature 428, 929–932.
Fernández, E., Boyd, P.W., Holligan, P.M., Harbour, D.S., 1993. Production of organic and inorganic carbon within a large-scale coccolithophore bloom in the northeast Atlantic Ocean. Marine Ecology Progress Series 97, 271–285.
Fernández, E., Fritz, J.J., Balch, W.M., 1996. Chemical composition of the coccolithophorid *Emiliania huxleyi* under light-limited steady state growth. Journal of Experimental Biology and Ecology 207, 149–160.
François, R., Honjo, S., Kirshfield, R., Manganini, S.J., 2002. Factors controlling the flux of organic carbon to the bathypelagic zone of the ocean. Global Biogeochemical Cycles 16, 1–20.
Frankignoulle, M., Canon, C., Gattuso, J.-P., 1994. Marine calcification as a source of carbon dioxide: positive feedback of increasing atmospheric $CO_2$. Limnology and Oceanography 39, 458–462.
Frankignoulle, M., Borges, A.V., 2001. European continental shelf as a significant sink for atmospheric carbon dioxide. Global Biogeochemical Cycles 15, 569–576.
Fuhrman, J.A., Azam, F., 1982. Thymidine incorporation as a measure of heterotrophic bacterioplanktion production in marine surface waters: evaluation and field results. Marine Biology 66, 109–120.
Garcia-Soto, C., Fernández, E., Pingree, R.D., Harbour, D.S., 1995. Evolution and structure of a shelf coccolithophore bloom in the western English channel. Journal of Plankton Research 17, 2011–2036.
Garcia-Soto, C., Pingree, R.D., 2009. Spring and summer blooms of phytoplankton (SeaWiFS/MODIS) along a ferry line in the Bay of Biscay and western English channel. Continental Shelf Research 29, 1111–1122.
Gattuso, J.-P., Frankignoulle, M., Wollast, R., 1998. Carbon and carbonate metabolism in coastal aquatic ecosystems. Annual Review of Ecology, Evolution and Systematics 29, 405–434.
Gazeau, F., Middelburg, J.J., Loijens, M., Vanderborght, J.-P., Pizay, M.-D., Gattuso, J.-P., 2007. Planktonic primary production in estuaries: comparison of $^{14}C$, $O_2$ and $^{18}O$ methods. AME 46, 95–106.
Grasshoff, K., Ehrhardt, M., Kremling, K., 1983. Methods of Seawater Analysis. Verlag Chemie, Weinheim.
GREPMA, 1988. Satellite (AVHRR:NOAA-9) and ship studies of a coccolithophorid bloom in the western English channel. Marine Nature 1, 1–14.
Harlay, J., De Bodt, C., Engel, A., Jansen, S., d'Hoop, Q., Piontek, J., Van Oostende, N., Groom, S.B., Sabbe, K., Chou, L., 2009. Abundance and size distribution of transparent exopolymer particles (TEP) in a coccolithophorid bloom in the northern Bay of Biscay. Deep Sea Research Part I 56, 1251–1265.
Harlay, J., Borges, A.V., van der Zee, C., Delille, B., Godoi, R.H.M., Schiettecatte, L.-S., Roevros, N., Aerts, K., Lapernat, P.-E., Rebreanu, L., Groom, S.B., Daro, M.-H., Van Grieken, R., Chou, L., 2010. Biogoechemical study of a coccolithophore bloom in the northern Bay of Biscay (NE Atlantic Ocean) in June 2004. Progress in Oceanography 86, 317–336.
Head, R.N., Crawford, D.W., Egge, J.K., Harris, R.P., Kristiansen, S., Lesley, D.J., Marañón, E., Pond, D., Purdie, D.A., 1998. The hydrography and biology of a bloom of the coccolithophorid *Emiliania huxleyi* in the northern North Sea. Journal of Sea Research 39, 255–266.
Hofmann, M., Schellnhuber, H.-J., 2009. Oceanic acidification affects marine carbon pump and triggers extended marine oxygen holes. Proceedings of the National Academy of Sciences 106, 3017–3022.
Holligan, P.M., Viollier, M., Harbour, D.S., Camus, P., Champagne-Philippe, M., 1983. Satellite and ship studies of coccolithophore production along a continental shelf edge. Nature 304, 339–342.
Holligan, P.M., Fernández, E., Aiken, W., Balch, W.M., Boyd, P.W., Burkill, P.H., Finch, M., Groom, S.B., Malin, G., Muller, K., Purdie, D.A., Robinson, C., Trees, C.C., Turner, S.M., van der Wal, P., 1993. A biogeochemical study of the coccolithophore, *Emiliania huxleyi*, in the North Atlantic. Global Biogeochemical Cycles 7, 879–900.
Huthnance, J.M., Coelho, H., Griffiths, C.R., Knight, P.J., Rees, A.P., Sinha, B., Vangriesheim, A., White, M., Chatwin, P.G., 2001. Physical structures, advection and mixing in the region of Goban spur. Deep Sea Research Part II 48, 2979–3021.
Hydes, D.J., Le Gall, A.C., Miller, A.E.J., Brockmann, U., Raabe, T., Holley, S., Alvarez-Salgado, X., Antia, A.N., Balzer, W., Chou, L., 2001. Supply and demand of nutrients and dissolved organic matter at and across the NW European shelf break in relation to hydrography and biogeochemical activity. Deep Sea Research Part II 48, 3023–3047.
Joassin, P., Delille, B., Soetaert, K., Borges, A.V., Chou, L., Engel, A., Gattuso, J.-P., Harlay, J., Riebesell, U., Suykens, K., Gregoire, M., 2008. A mathematical modelling of bloom of the coccolithophore *Emiliania huxleyi* in a mesocosm experiment. Biogeosciences Discuss 5, 787–840.
Joint, I., Wollast, R., Chou, L., Batten, S., Elskens, M., Edwards, E.S., Hirst, A., Burkill, P.H., Groom, S.B., Gibb, S.W., Miller, A., Hydes, D.J., Dehairs, F., Antia, A.N., Barlow, R., Rees, A., Pomroy, A., Brockmann, U., Cimmings, D., Lampitt, R., Loijens, M., Mantoura, F., Miller, P., Raabe, T., Alvarez-Salgado, X., Stelfox, C., Woolfenden, J., 2001. Pelagic production at the Celtic Sea shelf break. Deep Sea Research Part II 48, 3049–3081.
Kahl, L.A., Vardi, A., Schofield, O., 2008. Effects of phytoplankton physiology on export flux. Marine Ecology Progress Series 354, 3–19.
Kirchman, D.L., 1992. Incorporation of thymidine and leucine in the subarctic Pacific: application to estimating bacterial production. Marine Ecology Progress Series 82, 301–309.
Knap, A.H., Michaels, A.E., Close, A., Ducklow, H.W., Dickson, A.G., 1996. Protocols for the Joint Global Ocean Flux Study (JGOFS) core measurements. Report no 19. Bergen, Norway, UNESCO. JGOFS Report.
Koeve, W., 2005. Magnitude of excess carbon sequestration into the deep ocean and the possible role of TEP. Marine Ecology Progress Series 291, 53–64.
Lessard, E.J., Merico, A., Tyrrell, T., 2005. Nitrate: phosphate ratios and *Emiliania huxleyi* blooms. Limnology and Oceanography. 50, 1020–1024.
Logan, B.E., Passow, U., Alldredge, A.L., Grossart, H.-P., Simon, M., 1995. Rapid formation and sedimentation of large aggregates is predictable from coagulation rates (half-lives) of transparent exopolymer particles (TEP). Deep Sea Research Part II 42, 203–214.
Marañón, E., González, N., 1997. Primary production, calcification and macromolecular synthesis in a bloom of the coccolithophore *Emiliania huxleyi* in the North Sea. Marine Ecology Progress Series 157, 61–77.
Margalef, R. 1997. Our Biosphere, Oldendorf/Luhe, Germany.
Marra, J., 2002. Approaches to the measurement of plankton production. In: Williams, P.J.l.B., Thomas, D.N., Reynolds, C.S. (Eds.), Phytoplankton Productivity: Carbon Assimilation in Marine and Freshwater Ecosystems. Blackwell, Cambridge, pp. 78–108.
Murata, A., Takizawa, T., 2002. Impact of a coccolithophorid bloom on the $CO_2$ system in surface waters of the eastern Bering Sea shelf. Geophysical Research Letters 29, 1547.
Nanninga, H.J., Tyrrell, T., 1996. Importance of light for the formation of algal blooms by *Emiliania huxleyi*. Marine Ecology Progress Series 136, 195–203.
Nimer, N.A., Brownlee, C., Merrett, M.J., 1994. Carbon dioxide availability, intracellular pH and growth rate of the coccolithophore *Emiliania huxleyi*. Marine Ecology Progress Series 109, 257–262.
Orr, J.C., Fabry, V.J., Aumont, O., Bopp, L., Doney, S.C., Feely, R.A., Gnanadesikan, A., Gruber, N., Ishida, A., Joos, F., Key, R.M., Lindsay, K., Maier-Reimer, E., Matear, R., Monfray, P., Mouchet, A., Najjar, R.G., Plattner, G.-K., Rodgers, K.B., Sabine, C.L., Sarmiento, J.L., Schlitzer, R., Slater, R.D., Totterdell, I.J., Weirig, M.-F., Yamanaka, Y., Yool, A., 2005. Anthropogenic ocean acidification over the twenty-first century and its impact on calcifying organisms. Nature 437, 681–686.
Paasche, E., 1973. Silicon and the ecology of marine plankton diatoms. II. silicate-uptake kinetics in five diatom species. Marine Biology 19, 262–269.
Passow, U., 2002. Transparent exopolymer particles (TEP) in aquatic environments. Progress in Oceanography 55, 287–333.
Pingree, R.D., 1993. Flow of surface waters to the west of the British Isles and in the Bay of Biscay. Deep Sea Research Part II 40, 369–388.
Pingree, R.D., Le Cann, B., 1989. Celtic and Armorican shelf and slope residual currents. Progress in Oceanography 23, 303–338.
Pingree, R.D., Mardell, G.T., New, A.L., 1986. Propagation of internal tides from the upper slopes of the Bay of Biscay. Nature 321, 154–158.
Pingree, R.D., New, A.L., 1995. Structure, seasonal development and sunglint spatial coherence of the internal tide on the Celtic and Armorican shelves and in the Bay of Biscay. Deep Sea Research Part I 42, 245–284.
Pingree, R.D., Sinha, B., Griffiths, C.R., 1999. Seasonality of the European slope current (Goban Spur) and ocean margin exchange. Continental Shelf Research 19, 929–975.
Purdie, D.A., Finch, M., 1994. The impact of a coccolithophorid bloom on dissolved carbon dioxide in sea water enclosures in a Norwegian Fjord. Sarsia 79, 379–387.
Rees, A.P., Woodward, E.M., Robinson, C., Cummings, D.G., Tarran, G.A., Joint, I., 2002. Size-fractionated nitrogen uptake and carbon fixation during a developing coccolithophore bloom in the North Sea during June 1999. Deep Sea Research Part II 49, 2905–2927.
Riebesell, U., Zondervan, I., Rost, B., Tortell, P.D., Zeebe, R.E., Morel, F.M.M., 2000. Reduced calcification of marine plankton in response of increased atmospheric $CO_2$. Nature 407, 364–367.
Riebesell, U., Schulz, K.G., Bellerby, R.G.J., Botros, M., Fritsche, P., Meyerhofer, M., Neill, C., Nondal, G., Oschlies, A., Wohlers, J., Zollner, E., 2007. Enhanced biological carbon consumption in a high $CO_2$ ocean. Nature 450, 545–548.
Riegman, R., Stolte, W., Noordeloos, A.A.M., Slezak, D., 2000. Nutrient uptake and alkaline phosphatase (ec 3:1:3:1) activity of *Emiliania huxleyi* (prymnesiophyceae) during growth under N and P limitation in continuous cultures. Journal of Phycology 36, 87–96.
Robertson, J.E., Robinson, C., Turner, D.R., Holligan, P., Watson, A.J., Boyd, P.W., Fernández, E., Finch, M., 1994. The impact of a coccolithophore bloom on oceanic

carbon uptake in the northeast Atlantic during summer 1991. Deep Sea Research Part I 41, 297–314.

Robinson, C., Widdicombe, C.E., Zubkov, M.V., Tarran, G.A., Miller, A.E.J., Rees, A.P., 2002. Plankton community respiration during a coccolithophore bloom. Deep Sea Research Part II 49, 2929–2950.

Rost, B., Riebesell, U., 2004. Coccolithophores and the biological pump: responses to environmental changes. In: Thierstein, H.R., Young, J.R. (Eds.), Coccolithophores. From Molecular Processes to Global Impact, pp. 99–127.

Sciandra, A., Harlay, J., Lefèvre, D., Lemée, R., Rimmelin, P., Denis, M., Gattuso, J.-P., 2003. Response of coccolithophorid *Emiliania huxleyi* to elevated partial pressure of $CO_2$ under nitrogen limitation. Marine Ecology Progress Series 261, 111–122.

Sharples, J., Tweddle, J.F., Green, J.A.M., Palmer, M.R., Kim, Y.-N., Hickman, A.E., Holligan, P.M., Moore, C.M., Rippeth, T.P., Simpson, J.H., Krivtsov, V., 2007. Spring-neap modulation of internal tide mixing and vertical nitrate fluxes at a shelf edge in summer. Limnology and Oceanography 52, 1735–1747.

Sharples, J., Moore, C.M., Hickman, A.E., Holligan, P.M., Tweddle, J.F., Palmer, M.R., Simpson, J.H., 2009. Internal tidal mixing as a control on continental nmargin ecosystems. Geophysical Research Letters 36, L23603.

Smith, W.H., Sandwell, D.T., 1997. Global sea floor topography from satellite altimetry and ship depth soundings. Science 277, 1956–1962.

Suykens, K., Delille, B., Chou, L., De Bodt, C., Harlay, J., Borges, A.V., 2010a. Dissolved inorganic carbon dynamics and air–sea carbon dioxide fluxes during coccolithophorid blooms in the Northwest European continental margin (northern Bay of Biscay). Global Biogeochemical Cycles 24, GB3022. doi:10.1029/2009GB003730.

Suykens, K., Schmidt, S., Delille, B., Chou, L., De Bodt, C., Harlay, J., Fagel, N., Borges, A.V. 2010b. Benthic remineralization in the northwest European continental margin (northern Bay of Biscay). Continental Shelf Research, Submitted for publication.

Van den Meersche, K., Soetaert, K., Middelburg, J.J., 2008. A Bayesian compositional estimator for microbial taxonomy based on biomarkers. Limnology and Oceanography Methods 6, 190–199.

van der Wal, P., Kempers, R.S., Veldhuis, M.J.W., 1995. Production and downward flux of organic matter and calcite in a North Sea bloom of the coccolithophore *Emiliania huxleyi*. Marine Ecology Progress Series 126, 247–265.

Wollast, R., Chou, L., 2001. The carbon cycle at the ocean margin in the northern Gulf of Biscay. Deep Sea Research Part II 48, 3265–3293.

Wright, S.W., Jeffrey, S.W., 1997. High-resolution HPLC system for chlorophylls and carotenoids of marine phytoplankton. In: Jeffrey, S.W., Mantoura, R.F.C., Wright, S.W. (Eds.), Phytoplankton pigments in oceanography. UNESCO Publishing, pp. 327–341.

Yentsch, C.S., Menzel, D.W., 1963. A method for the determination of phytoplankton chlorophyll and phaeophytin by fluorescence. Deep Sea Research and Oceanographic Abstracts 10, 221–231.